in silico Plants Vol. 4, No. 1, pp. 1–28
https://doi.org/10.1093/insilicoplants/diab038
Advance Access publication 18 January 2022
Special Issue: Functional-Structural Plant Models
Review

in silico Plants

OXFORD

On the pivotal role of water potential to model plant physiological processes

Tom De Swaef[1,*], Olivier Pieters[1,2], Simon Appeltans[3], Irene Borra-Serrano[1], Willem Coudron[1,4], Valentin Couvreur[5], Sarah Garré[1,6], Peter Lootens[1], Bart Nicolaï[7], Leroi Pols[7], Clément Saint Cast[5], Jakub Šalagovič[7], Maxime Van Haeverbeke[8], Michiel Stock[8] and Francis wyffels[2]

[1]Plant Sciences Unit, Flanders Research Institute for Agriculture Fisheries and Food (ILVO), 9090 Melle, Belgium
[2]IDLab-AIRO – Ghent University – imec, 9052 Zwijnaarde, Belgium
[3]Department of Plants and Crops, Ghent University, 9000 Gent, Belgium
[4]Department of Environment, Ghent University, 9000 Gent, Belgium
[5]Earth and Life Institute, University of Louvain, 1348 Louvain-La-Neuve, Belgium
[6]Gembloux Agro-Bio Tech, Liège University, 5030 Gembloux, Belgium
[7]Division of Mechatronics, Biostatistics and Sensors (MeBioS), KU Leuven, 3001 Leuven, Belgium
[8]Department of Data Analysis and Mathematical Modelling, Ghent University, 9000 Gent, Belgium
*Corresponding author's e-mail address: tom.deswaef@ilvo.vlaanderen.be

Guest Editor: Katrin Kahlen

Editor-in-Chief: Stephen P. Long

Citation: De Swaef T, Pieters O, Appeltans S, Borra-Serrano I, Coudron W, Couvreur V, Garré S, Lootens P, Nicolaï B, Pols L, Saint Cast C, Šalagovič J, Van Haeverbeke M, Stock M, Wyffels F. 2022. On the pivotal role of water potential to model plant physiological processes. *In Silico Plants* **2022**: diab038; doi: 10.1093/insilicoplants/diab038

ABSTRACT

Water potential explains water transport in the soil–plant–atmosphere continuum (SPAC), and is gaining interest as connecting variable between 'pedo-, bio- and atmosphere'. It is primarily used to simulate hydraulics in the SPAC, and is thus essential for studying drought effects. Recent implementations of hydraulics in large-scale terrestrial biosphere models (TBMs) improved their performance under water-limited conditions, while hydraulic features of recent detailed functional–structural plant models (FSPMs) open new possibilities for dissecting complex traits for drought tolerance. These developments in models across scales deserve a critical appraisal to evaluate its potential for wider use in FSPMs, but also in crop systems models (CSMs), where hydraulics are currently still absent. After refreshing the physical basis, we first address models where water potential is primarily used for describing water transport along the transpiration pathway from the soil to the leaves, through the roots, the xylem and the leaf mesophyll. Then, we highlight models for three ecophysiological processes, which have well-recognized links to water potential: phloem transport, stomatal conductance and organ growth. We identify water potential as the bridge between soil, root and shoot models, as the physiological variable integrating below- and above-ground abiotic drivers, but also as the link between water status and growth. Models making these connections enable identifying crucial traits for ecosystem resilience to drought and for breeding towards improved drought tolerance in crops. Including hydraulics often increases model complexity, and thus requires experimental data on soil and plant hydraulics. Nevertheless, modelling hydraulics is insightful at different scales (FSPMs, CSMs and TBMs).

KEYWORDS: crop model; drought stress; FSPM; plant hydraulics; plant growth; stomatal conductance.

1. INTRODUCTION

Water forms the basis of all life on earth, including plants. **Water** uptake and transpiration by plants are major components of the terrestrial water cycle, as plant transpiration accounts for 80–90 % of terrestrial evapotranspiration and returns about 30 % of the terrestrial precipitation back in the atmosphere (Beerling and Franks 2010; Jasechko *et al.* 2013). The main regulators of transpiration, the stomata, are also the main entrance for CO_2 uptake and thus link transpiration to photosynthesis. Furthermore, up to 95 % of plant fresh weight consists of water. Therefore, the uptake, transport and transpiration of this precious fluid are closely connected to plant productivity and survival (Choat *et al.* 2018). Unlike animals, plants are sessile organisms and thus have to fulfil their water requirements with the available water in their surrounding environment. As a result of this constraint, plants develop complex networks of tissues for water uptake, transportation and storage. Moreover, plants even adjust their growth cycle and phenology to seasonal variations in water availability, and build symbiotic alliances with microorganisms (Augé 2001). Studying **plant hydraulics** is, therefore, of major interest to better understand impacts of drought, but also salinity, which reduces the availability of water to the plant. This improved understanding is required to neutralize the attendant stresses to safeguard ecosystem functioning and agricultural production (Anderegg *et al.* 2012; Lesk *et al.* 2016; Martin-StPaul *et al.* 2017).

Water is vital for plants and impacts virtually every physiological mechanism. Consequently, effects of drought, and hydraulics in general, on productivity and survival consist of complex cross-mechanism interactions. In this respect, (mechanistic) **plant models** are powerful tools to capture and connect detailed knowledge on various plant physiological processes and provide more holistic insights. An extensive overview of plant models at different scales can be found on https://www.quantitative-plant.org/model. The modelling of water transport is increasingly important to assess the consequences of climate change, and particularly drought on crops (Parent and Tardieu 2014). Such models can help to understand and predict effects on plant growth and water relations in an unpredictable climate, but also to identify beneficial traits for improved resilience (Damour *et al.* 2010; Christoffersen *et al.* 2016; Anderegg *et al.* 2017; Carminati and Javaux 2020).

To understand the flow and function of water in plants and their direct environment (soil and atmosphere), the concept of **water potential** is essential. Water potential is a measure of the free energy of water per unit volume and explains the direction (downward gradient) and flow rate of water transport inside the soil–plant–atmosphere continuum (SPAC). Water potential is gaining interest as a connecting variable between 'pedo-, bio- and atmosphere' (Martínez-Vilalta *et al.* 2014; Steppe 2018; Carminati and Javaux 2020; Charrier 2020).

Most **models that explicitly include water potential** and waters transport have focused on enhancing understanding of detailed hydraulic mechanisms in plants, especially in trees (Fatichi *et al.* 2016; Mencuccini *et al.* 2019). However, recent developments in the vegetation modelling community have highlighted the importance of including hydraulics in large-scale terrestrial biosphere models (TBMs) to improve model performance, especially under drought or saline conditions (Anderegg and Venturas 2020; Eller *et al.* 2020; Sabot *et al.* 2020). Furthermore, several functional–structural plant models (FSPMs) include hydraulics in a three-dimensional root (Javaux *et al.* 2008; Postma *et al.* 2017; Schnepf *et al.* 2018), shoot (Dauzat *et al.* 2001; da Silva *et al.* 2011; Nikinmaa *et al.* 2014; Coussement *et al.* 2020), or whole-plant (Zhou *et al.* 2020) architecture to simulate within-plant spatial and temporal variations in water uptake, transport and transpiration. Moreover, besides the water flow along the soil–plant–atmosphere pathway, water potential has been mathematically linked to other plant processes like phloem transport (Daudet *et al.* 2002), stomatal conductance (Anderegg and Venturas 2020) and plant growth dynamics (Coussement *et al.* 2020). These recent applications of hydraulics in TBMs and FSPMs have thus enhanced model robustness and yielded novel insights. Although implementations of hydraulics in models are on the rise, they are not yet widespread. This is especially true for crop systems models (CSMs) that typically operate at the field or farm scale (Jin *et al.* 2016; Tardieu *et al.* 2020). Especially for studying responses to drought, models at different scales (FSPM, CSM and TBM) might benefit from including hydraulics in their formalisms (Hoogenboom *et al.* 2021). Therefore, we believe the time is right to gather current model implementations of plant hydraulics, and to investigate how this links to other physiological plant processes in plant models.

Firstly, we briefly introduce the physical basis of water potential, how this is conceived in different scientific communities and how it drives water flow in the SPAC (Section 2). Then, we dive into literature on plant models that deal with water flow along the transpiration stream (Section 3), by dividing the path in functional entities: soil to root (Section 3.1), radial from root epidermis to root xylem (Section 3.2), vertical inside xylem (Section 3.3) and from leaf xylem to sites of evaporation (Section 3.4). Subsequently, we investigate how hydraulics are linked to other plant physiological processes in models like phloem transport (Section 4), stomatal conductance (Section 5.1) and plant growth (Section 5.2). In a first discussion (Section 6.1) we synthesize how water potential can serve as a central model variable that connects multiple ecophysiological mechanisms in plant models. Then, we revise the potential of hydraulically based models for identifying interesting phenotypic traits for drought tolerance (Section 6.2). Finally, we focus on pitfalls and potential solutions for dealing with model complexity, associated to including hydraulics in plant models (Section 6.3).

2. THE CONCEPT OF WATER POTENTIAL

Water status and transport in the SPAC are described thermodynamically by the water potential Ψ ([Pa]; Slatyer 1967). This measure has been derived from the chemical potential of water (μ_w; [J mol^{-1}]), which corresponds to the change in free energy of water in a system, relative to the moles of water added to it (Tyree and Zimmermann 2002):

$$\mu_w = \mu_{w,0} - V_w \cdot \Pi + V_w \cdot P - V_w \cdot M + M_w \cdot g \cdot z, \quad (2.1)$$

where $\mu_{w,0}$ is the chemical potential for a specific reference state [J mol^{-1}]. This reference state is typically the state of pure water at sea level at atmospheric pressure. V_w is the molal volume of pure water [18×10^{-6} m^3 mol^{-1}], Π is the osmotic pressure [Pa], P is the hydrostatic pressure [Pa], M is the matric suction due to the attraction by solids [Pa], M_w is the molar mass of water [18×10^{-3} kg mol^{-1}], g is the gravitational acceleration [N kg^{-1}] and z is the vertical height

compared to the reference state [m]. In plant physiology, μ_w is commonly converted to pressure units to obtain Ψ in [Pa], although values of Ψ are typically in the range of kPa or MPa in the SPAC (H. G. Jones 2015):

$$\Psi = \frac{\mu_w - \mu_{w,0}}{V_w} = P - \Pi - M + \rho_w \cdot g \cdot z, \tag{2.2}$$

with ρ_w the density of water [kg m^{-3}]. Equation (2.2) shows four additive components, representing the four forces that act on water molecules:

$$\Psi = \Psi^p + \Psi^\pi + \Psi^\tau + \Psi^g \tag{2.3}$$

The hydrostatic potential ($\Psi^p = P$) describes the difference in hydrostatic pressure from the reference. Inside living cells (i.e. the symplast), this generally takes a positive value corresponding with the turgor pressure. Inside the cell walls or xylem vessels (i.e. the apoplast), this corresponds to the tension generated via transpiration and is generally negative, except in the presence of root pressure. The osmotic potential ($\Psi^\pi = -\Pi$) results from osmotically active solutes in the water. This component is always negative, with a magnitude proportional to the solute concentration (c_s; [mol m^{-3}]) and the absolute temperature (T; [K]). A common approximation for Ψ^π is given by the van't Hoff equation:

$$\Psi^\pi = -\Re \cdot T \cdot c_s \tag{2.4}$$

where $\Re$ is the universal gas constant [8.31 J mol^{-1} K^{-1}]. This equation holds for diluted solutions, but, e.g., for phloem cells, where solute concentrations can be higher, Thompson and Holbrook (2003) suggest an empirical adaptation to this formula, based on Michel (1972):

$$\Psi^\pi = -\rho_w \cdot \Re \cdot T \cdot (0.998m + 0.089m^2), \tag{2.5}$$

where m is the molality of the solution [mol kg^{-1}]. The component for matric potential ($\Psi^\tau = M$) originates from the interaction of water with a solid matrix like soil particles or cell walls through hydrogen bonding and other local forces. Terminology of matric potential differs between soil and plant science. In soil science, matric potential is considered as the (negative) pressure that can be measured using soil tensiometers and is, therefore, identical to what plant scientists consider as hydrostatic water potential Ψ^p (Nobel 1983; Hunt *et al.* 1991; Tyree 2003). In plant science, matric potential Ψ^τ is restricted to short-range interaction effects between water and a solid surface (like cell walls), whereas other interactions with the solid phase like the capillary effects and the development of concave menisci are included in the hydrostatic part of the thermodynamic derivation. These short-range effects influence only a small fraction of the total water in plants and are generally omitted or included in the osmotic potential Ψ^π (Briggs 1967; Passioura 1980; H. G. Jones 2015).

Finally, the gravitational component ($\Psi^g = \rho_w \cdot g \cdot z$) is relevant for large trees, as Ψ^g increases with about 0.01 MPa per meter of height.

The above expressions for water potential are valid for all sites in the SPAC where water is in the liquid phase (soil, rhizosphere, roots, stems, buds, flowers, fruits and leaves). For water in the gaseous phase, important in soil (especially near the surface where evaporation takes place; Or *et al.* 2013), in the substomatal cavity of the leaf, at the leaf surface and in the atmosphere, water potential is expressed by the equation of Spanner (1951):

$$\Psi = \frac{\Re T}{V_w} \cdot log\left(\frac{e}{e_0}\right), \tag{2.6}$$

where and e_0 and e are the saturated water vapour pressure [Pa] and the actual water vapour pressure [Pa], respectively. An overview of water potential components in different sites of the SPAC is presented in Table 1.

Throughout this review, we will use consistent units to describe numerical quantities (Table 1), using the SI units throughout. However, when alternative units are prevalent in literature, they are also included. It is quite common that different scientific communities use distinct units for the same component, depending on their affinities.

Following Darcy's law (1856), the volumetric water flow J_v [m^3 s^{-1}] between two sites in the SPAC is directed towards the site with the lower Ψ and proportional to the difference in Ψ ($\Delta\Psi$) between them:

$$J_v = K \cdot \Delta\Psi, \tag{2.7a}$$

Table 1. Overview of symbols and units for water potential components used throughout this review. Note that matric potential as used in soil and plant communities do not encompass entirely the same processes.

Symbol	Description	Sign	Influencing factors
Ψ	Water potential	+/−	
Plant—liquid phase			
Ψ^p	Hydrostatic potential	+/−	Turgor, capillary forces
Ψ^π	Osmotic potential	−	Solute concentration, temperature
Ψ^τ	Matric potential	−	Bonding forces by cell walls on water
Ψ^g	Gravitation potential	+/−	Height
Soil–plant–atmosphere—gaseous phase			
Ψ	Water potential	+/−	Vapour pressure deficit, temperature
Soil—liquid phase			
Ψ^p	Hydrostatic potential	+/−	Water column or externally applied suction
Ψ^π	Osmotic potential	−	Solute concentration, temperature
Ψ^τ	Matric potential	−	Capillary forces and adhesive forces of porous matrix
Ψ^g	Gravitational potential	+/−	Height

$$J_v = \frac{\Delta\Psi}{R}, \tag{2.7b}$$

where K is hydraulic conductance [m^3 MPa^{-1} s^{-1}], and R ($=1/K$) is hydraulic resistance [MPa s m^{-3}]. Although this is a very simple representation of water transport, it serves as a base equation on which more complex derivations have been built. Adaptations depend on the system under study in terms of scale and tissue characteristics (Carminati and Javaux 2020). Many of these will be discussed in the following sections, but in general, hydraulic conductance K can be broken down into four components (Darcy 1856):

$$K = \frac{k \cdot A}{\eta \cdot L}, \tag{2.8}$$

where the permeability k is an intrinsic characteristic of the porous medium (soil or plant tissue) [m^2], A is the cross-sectional area of the medium perpendicular to the flow direction [m^2], η is the dynamic viscosity the watery solution [MPa s] and L is the path length [m]. As mentioned above, usage of terminology and units may differ between scientific community. In soil science, the use of 'conductivity' is more common than the use of 'conductance'. Although soil scientists use the same symbol K, this actually only includes the k and η of equation (2.8). Here we will use κ for hydraulic 'conductivity' and K for hydraulic 'conductance' such that:

$$\kappa = \frac{k}{\eta} \tag{2.9}$$

This would result in units [m^2 MPa^{-1} s^{-1}]. However, in soil science, water potential is most often expressed in length units [m], and is called 'hydraulic head' H, referring to the pressure exerted by a water column with height H [m] on a surface:

$$\Psi = \rho_w \cdot g \cdot H \tag{2.10}$$

Consequently, the unit of κ most often used in soil science is [m s^{-1}], thereby including ρ_w and g. Because of equation (2.9), κ depends on the temperature (through the viscosity η) and on the intrinsic geometry of the porous material (through the permeability k), where the latter may refer to soil or plant tissues. The conductance K also takes into account the specific dimensions of the medium in terms of area A and path length L. In studies on plant hydraulics, intermediate variables have been used, taking only area into account (Martre and Durand 2001). Other variations also exist in the use of variables for water quantity (volume [m^3] or mass [kg]), volumetric water flow (flux J_v [m^3 s^{-1}] or flux density q [m^3 m^{-2} s^{-1}]) (Hunt *et al.* 1991). It is of great significance that units and variables are properly rescaled when linking water flow across different research domains. In Table 2 we list all symbols and abbreviations, used in the manuscript.

Table 2. Overview of the symbols, descriptions and (generalized) units of variables and parameters used in this review.

Symbol	Unit	Description
a	MPa^{-1}	Curvature parameter for *PLC* curve
a_{ABA}	m s^{-1}	Sensitivity of leaf elongation rate to xylem abscisic acid concentration
a_{LER}	m s^{-1}	Maximum leaf elongation rate
[ABA]	Dimensionless	Abscisic acid concentration
c_{LER}	MPa^{-1}	Sensitivity of leaf elongation rate to xylem water potential
c_s	mol m^{-3}	Solute concentration
d_1	kPa^{-1}	Empirical coefficient in BBL models of stomatal conductance
e	Pa or kPa	(Actual) vapour pressure
e_0	Pa or kPa	Saturated vapour pressure
g	N kg^{-1}	Gravitational acceleration
g_{b_l}	m s^{-1}	Boundary-layer conductance
g_c	m s^{-1}	Cuticular conductance
g_s	m s^{-1}	Stomatal conductance
$g_{s,max}$	m s^{-1}	Maximum stomatal conductance
$g_{s,0}$	m s^{-1}	Minimum stomatal conductance
$g_{s,1}$	m^3 ppm mol^{-1}	Empirical coefficient in BBL models of stomatal conductance
k	m^2	Hydraulic permeability
k_g	s^{-1}	Growth coefficient
m	mol kg^{-1}	Solution molality
n	Dimensionless	Number of conduits in the xylem cross-section
p	Dimensionless	Shape factor
q	m^3 m^{-2} s^{-1}	Water flux density
q_m	m s^{-1}	Water flux density across the plasma membrane
r	m	Xylem conduit radius
s_1, s_2, s_3	MPa^{-1}	Shape factors in stomatal models
t	s	Time
z	m	Vertical height compared to the reference state
A	m^2	Cross-sectional area perpendicular to the flow path
A_n	mol CO_2 m^{-2} s^{-1}	Net photosynthesis rate
$[C]$	Dimensionless	Carbon substrate concentration
$[C_a]$	ppm	CO_2 concentration of the air at the leaf surface
E	m s^{-1}	Transpiration rate
H	m	Hydraulic pressure head
J_v	m^3 s^{-1}	Volumetric water flow rate
K	m^3 MPa^{-1} s^{-1}	Hydraulic conductance
K_{leaf}	m^3 MPa^{-1} s^{-1}	Leaf hydraulic conductance
K_{ox}	m^3 MPa^{-1} s^{-1}	Outside-xylem leaf hydraulic conductance
K_{root}	m^3 MPa^{-1} s^{-1}	Radial root hydraulic conductance
K_{soil}	m^2 s^{-1}	Soil hydraulic conductance

3. MODELLING WATER TRANSPORT ALONG THE TRANSPIRATION PATH

The major and most straightforward application of water potential in plant models is to study the water flow driven by transpiration, in

Table 2. Continued

Symbol	Unit	Description
$K_{soil,0}$	$m^2\ s^{-1}$	Saturated soil hydraulic conductance
K_{tot}	$m^3\ MPa^{-1}\ s^{-1}$	Total hydraulic conductance of the water transport path from soil to leaf
K_{xylem}	$m^3\ MPa^{-1}\ s^{-1}$	Xylem hydraulic conductance
$K_{xylem,i}$	$m^3\ MPa^{-1}\ s^{-1}$	Hydraulic conductance of xylem conduit *i*
L	m	Path length
LER	$m\ s^{-1}$	Leaf elongation rate
M	MPa	Matric suction due to the attraction by solids
M_w	18×10^{-3} kg mol^{-1}	Molar mass of water
$[N]$	Dimensionless	Nitrogen substrate concentration
P	MPa	Hydrostatic pressure
PLC	Dimensionless	Percentage loss of conductance
Q_p	$m^{-2}\ s^{-1}$	Photosynthetically active radiation
R	$MPa\ s\ m^{-3}$	Hydraulic resistance
R_{tot}	$MPa\ s\ m^{-3}$	Total hydraulic resistance of the water transport path from soil to leaf
S	s^{-1}	Sink term
T	K	Absolute temperature
T_{leaf}	K	Absolute temperature
V	m^3	Cell or tissue volume
V_w	$18 \times 10^{-6}\ m^3$ mol^{-1}	Molal volume of water
W	$kg\ m^{-2}$	Dry matter mass per area
Y	MPa	Threshold turgor pressure for growth
β	Dimensionless	Sensitivity factor to abscisic acid concentration
δe	kPa	Vapour pressure deficit
ε	MPa	Elastic modulus
η	MPa s	Dynamic viscosity of the solution
ϕ	$MPa^{-1}\ s^{-1}$	Cell wall extensibility
κ	$m\ s^{-1}$	Hydraulic conductivity
κ_m	$m\ MPa^{-1}\ s^{-1}$	Membrane hydraulic conductivity
κ_{soil}	$m\ s^{-1}$	Soil hydraulic conductivity
$\kappa_{soil,0}$	$m\ s^{-1}$	Saturated soil hydraulic conductivity
λ	mol CO_2 m^{-3} H_2O	Marginal water use efficiency
μ_w	$J\ mol^{-1}$	Chemical potential of water
$\mu_{w,0}$	$J\ mol^{-1}$	Chemical potential of water for a reference state
ρ_w	$kg\ m^{-3}$	Density of water
σ	Dimensionless	Reflection coefficient
θ	$m^3\ m^{-3}$	Volumetric water content
Γ	ppm	CO_2 compensation point
Π	MPa	Osmotic pressure
Ψ	MPa	Total water potential
Ψ^g	MPa	Gravitational water potential
Ψ^p	MPa	Hydrostatic water potential
Ψ_c^p	MPa	Hydrostatic water potential in the cytosol

Table 2. Continued

Symbol	Unit	Description
Ψ_w^p	MPa	Hydrostatic water potential in the cell wall
Ψ^π	MPa	Osmotic water potential
Ψ_c^π	MPa	Osmotic water potential in the cytosol
Ψ_w^π	MPa	Osmotic water potential in the cell wall
Ψ^τ	MPa	Matric water potential
Ψ_{crit}	MPa	Critical water potential for growth
Ψ_{leaf}	MPa	Bulk leaf water potential
Ψ_{max}	MPa	Water potential at which response function equals 1
Ψ_{min}	MPa	Water potential at which response function is zero
Ψ_0	MPa	Reference leaf water potential in equation (5.3b)
$\Psi_{1/2}$	MPa	Water potential when stomatal conductance is reduced to half (equation (5.3a))
Ψ_{12}	MPa	Water potential when *PLC* equals 12 %
Ψ_{50}	MPa	Water potential when *PLC* equals 50 %
Ψ_{88}	MPa	Water potential when *PLC* equals 88 %
$\Re$	$8.31\ J\ mol^{-1}\ K^{-1}$	Universal gas constant

accordance with the cohesion-tension theory (H. H. Dixon and Joly 1895). This theory explains how water moves in the soil towards the root surface, from the root surface to the xylem, inside the xylem from the roots towards the leaves and outside the xylem in the leaves to the sites of transpiration (Fig. 1). The driving force of this upward flow is the surface tension formed by capillary forces at the air–water interface of the mesophyll cell walls in the leaves, pulling on the water column. The water column is considered to be under 'tension' as the bulk liquid pressure is below atmospheric pressure. A recent review by Venturas *et al.* (2017) presents a clear overview of the current knowledge on this water transport path. In the next sections we will focus on how water transport in the different parts of the SPAC is modelled, making use of water potential as a central variable.

3.1 Water transport from soil to root, across the rhizosphere

Soil is a porous medium in which water moves following gradients of water potential, just like in plants, as described above. Henry Darcy (1856) experimentally determined that the flux of water through a saturated isotropic porous medium could be expressed as the product of the conductance to flow, characterized by the medium, and forces acting to 'push' the fluid through the medium, very similar to equation (2.7) (Fig. 2). Darcy defined the following properties for saturated conditions:

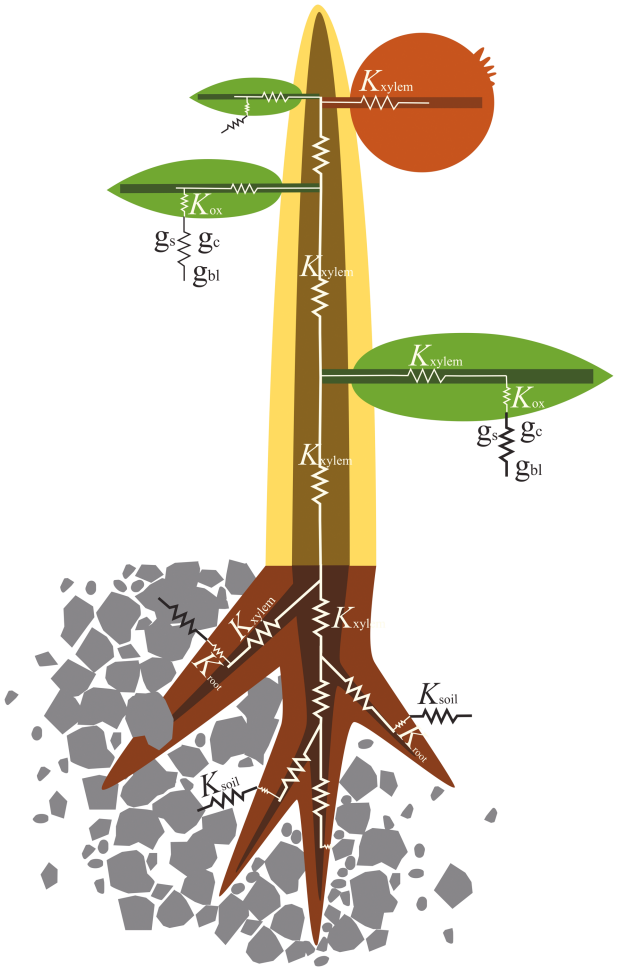

Figure 1. Scheme of water flow: (i) from the soil towards the root surface, (ii) from the root surface to the xylem, (iii) inside the xylem from the roots towards the leaves and (iv) outside the xylem in the leaves to the sites of transpiration. K_{soil}, K_{root}, K_{xylem}, K_{ox} are the respective hydraulic conductances. For completeness, conductance in the gaseous phase was included: stomatal conductance (g_s), cuticular conductance (g_c) and boundary-layer conductance (g_{bl}).

$$q = -\kappa_{soil,0} \cdot \frac{\Delta H}{L}, \tag{3.1a}$$

$$J_v = -K_{soil,0} \cdot \Delta H \tag{3.1b}$$

In soil physics, the flux density, q [$m^3\ m^{-2}\ s^{-1}$], is typically used instead of the flow rate, J_v [$m^3\ s^{-1}$]. $\kappa_{soil,0}$ and $K_{soil,0}$ are the saturated soil hydraulic conductivity [$m\ s^{-1}$] and conductance [$m^2\ s^{-1}$], respectively. ΔH is the difference in hydraulic head [m].

However, most flow processes in the field occur while the soil is unsaturated, or in the presence of an air phase. This situation drastically modifies water flow channels. As the water content decreases, the flow in the liquid phase is constrained to narrower and more tortuous

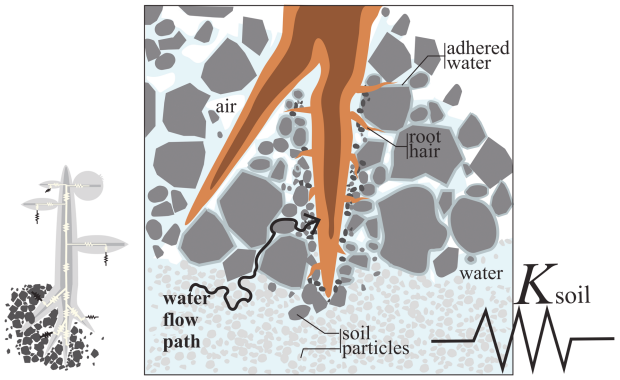

Figure 2. Scheme of water flow from the soil towards the roots, where K_{soil} is the soil hydraulic conductance. The dark region in the small image on the left indicates the location of the soil in the SPAC.

channels. Therefore, Buckingham *et al.* (1907) extended equation (3.1) to unsaturated flow by adding the main assumption that the unsaturated soil hydraulic conductivity κ_{soil} is a function of the water content, θ [$m^3\ m^{-3}$]. In Buckingham–Darcy's law for variably saturated flow the basic form is preserved as:

$$q = -\kappa_{soil}(\theta)\frac{\Delta H}{L} \tag{3.2}$$

A large number of models are built upon this equation, and the derived Richards equation (Richards 1931):

$$\frac{\partial \theta}{\partial t} = \frac{\partial}{\partial z}\left[\kappa_{soil}(\theta)\left(\frac{\partial H}{\partial z} + 1\right)\right] - S(z,t), \tag{3.3}$$

where $S(z,t)$ is the sink term [s^{-1}] representing root water uptake, which is a function of time t in [s] and elevation z in [m]. All these models are spatially explicit, because they calculate the flow of water across the path from the bulk soil towards the soil–root interface, but the number of dimensions for which they provide solutions varies from 1D (e.g. Gardner 1960; Simunek *et al.* 2005) to 3D (e.g. Javaux *et al.* 2013; Hammond *et al.* 2014). This sink term can vary from a fairly simple term determined by a root length density distribution to a dynamic term coming from an associated root water uptake model (Gardner 1960; Doussan *et al.* 2006; Javaux *et al.* 2013). More information on modelling frameworks for water flow in the soil is available on https://soil-modeling.org/resources-links/model-portal.

Historically, soil hydraulic conductivity is typically considered a function of porosity, which is most often linked to texture and bulk density as indirect proxies, via a so-called pedo-transfer function. However, the pore space determining the hydraulic conductivity is actually determined by soil structure and architecture, which are dynamic properties with multiscale facets. This is especially true for the rhizosphere, a thin zone around plant roots which is continuously influenced by plants and other organisms through exudation and other processes. Already in 1965, Cowan (1965) anticipated that the rhizosphere has hydraulic properties distinct from the bulk soil. More recently, factors like mucilage, a polymeric gel exuded by the roots, have

been included in hydraulic soil models to mechanistically capture the distinct hydraulic characteristics of the rhizosphere (Carminati 2012; Kroener *et al.* 2014). These models increasingly represent the rhizosphere as a dynamic environment, with variable hydraulic conductance. Recent modelling work has identified the hydraulic conductance of the soil–root interface as the primary constraint for plant water transport, especially in water-limited environments (Carminati and Javaux 2020; Javaux and Carminati 2021).

3.2 Water transport from root epidermis to xylem

Inside the root, water is transported radially from the soil–root interface to the xylem vessels through concentric layers of root cells: epidermis (a uniseriate layer of cells), exodermis (one or more cell layers situated adjacent to the epidermis), several layers of cortical cells, endodermis (one cell layer situated adjacent to the innermost layer of the cortex), pericycle and stelar parenchyma where root vascular tissues are located (Steudle and Peterson 1998) (Fig. 3). This composite structure offers three major radial pathways for transport of water: (i) the apoplastic path around the protoplast, where water and solutes can move towards the stele through free spaces and cell walls of the rhizodermis and cortex, (ii) the transmembrane pathway, where water (and solutes) move from apoplast to symplast and vice versa across cell membranes mediated by aquaporins and transporters localized in the cell membrane and (iii) the symplastic pathway, through plasmodesmata from one cell protoplast to the other using the cytoplasmic continuum (Peterson and Cholewa 1998; Steudle and Peterson 1998; Steudle 2000a, b). The symplastic and transmembrane pathways are often collectively referred to as the cell-to-cell pathway. Apoplastic water flow across the porous matrix of plant primary cell walls is driven by the same forces as soil water flow: gradients of summed gravitational and pressure potentials (Ψ^g and Ψ^p), although the gravitational component is generally negligible. The hydraulic conductivity is several orders of magnitude lower in cell walls than in soils, due to pore sizes as narrow as 5 nm (Carpita and Gibeaut 1993). The apoplastic pathway can be altered and eventually completely interrupted by the deposition of Casparian bands in endodermal and exodermal cell walls. These bands consist of suberin, and consequently force the water to exit the apoplast at least once on its journey towards the central cylinder.

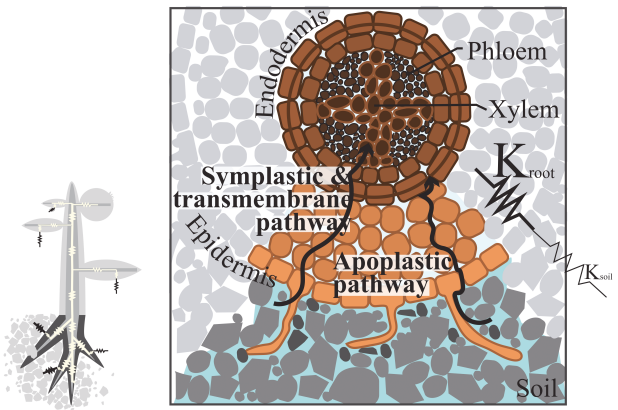

Figure 3. Scheme of water flow from the soil–root interface towards the xylem, across the root radius where K_{root} is the root radial hydraulic conductance. The dark region in the small image on the left indicates the location of the roots in the SPAC.

To exit the apoplast, water encounters another obstacle: the plasma membrane, a phospholipid bilayer with a hydrophobic centre. Nevertheless, water-specific transmembrane protein channels, aquaporins, allow the transport of up to 3×10^9 water molecules in a queue per second per aquaporin (de Groot and Grubmüller 2001). The presence of aquaporins increases the hydraulic conductivity of the membrane. Because the amount of aquaporins can be adjusted at a timescale of less than an hour, they offer the plant a means to actively modulate its tissue hydraulic conductance (Gambetta *et al.* 2017). The selectivity of membranes for solutes creates environments with different solute concentrations on opposite sides of the membrane, invoking osmotic potential differences (Ψ^π, see equation (2.4)). If solutes flow freely from one side to the other, the membrane is not selective and the osmotic potential difference across the membrane does not contribute to the driving force of water. In the opposite situation, if the membrane is only permeable for water (i.e. fully selective), the osmotic difference serves as an additional driving force. To capture the continuum of selectivity in transmembrane water transport in models, the reflection coefficient σ, ranging from zero if fully permeable to one if fully selective, is an elegant solution (Pusch and Woermann 1970):

$$q_m = \kappa_m \cdot (\Psi_w^p - \Psi_c^p + \sigma \cdot (\Psi_w^\pi - \Psi_c^\pi)), \tag{3.4}$$

where q_m [m s^{-1}] is the water flux density across the membrane, κ_m [m MPa^{-1} s^{-1}] is the membrane hydraulic conductivity, Ψ_w^p and Ψ_c^p [MPa] are the hydrostatic pressure potentials on the cell wall and cytosol side, respectively, and Ψ_w^π and Ψ_c^π [MPa] the (negative) osmotic potentials on the cell wall and cytosol sides, respectively. Note that the gravitational potential difference is zero horizontally, and, therefore, very often neglected.

In the third pathway, water flows between neighbouring cells without crossing their membranes and cell walls, through membranous sleeves connecting their cytosols directly: plasmodesmata. Plasmodesmata abundance varies across root tissues (Ma and Peterson 2001) and their aperture level can be regulated (Sevilem *et al.* 2013), thereby adjusting their hydraulic conductivity. Their aperture remains large enough for major solutes to freely flow with water (Bret-Harte and Silk 1994). Consequently, osmosis does not come into play and water is solely driven by hydrostatic pressure differentials along plasmodesmata. Equation (3.4) can be considered as a generalized form of equation (2.7) and can be applied to all three pathways of the composite model, where $\sigma = 0$ for the apoplastic and symplastic path, and $\sigma \in [0, 1]$ for the transmembrane path:

$$J_v = K \cdot (\Delta\Psi^p + \sigma \cdot (\Delta\Psi^\pi)) \tag{3.5}$$

These mechanisms have been used for modelling radial root water flow at multiple scales and dimensional complexities. In a first multiscale attempt, Zhu and Steudle (1991) proposed to attribute specific hydraulic conductivities and reflection coefficients to the apoplastic and cell-to-cell water pathways. Their parallel contributions, each taking the form of equation (3.5), were summed and shaped the total root

radial path. Further developments allowed the integration of varying hydraulic properties and suberization patterns along cell layers in a two-dimensional (radial–axial) hydraulic network (Zwieniecki *et al.* 2002) and the separation of cell walls and protoplasts for each individual cell (Foster and Miklavcic 2017). In parallel, Couvreur *et al.* (2018) developed a transverse two-dimensional model of subcellular water flow in root anatomical layouts digitized semi-automatically (Pound *et al.* 2012) or simulated (Heymans *et al.* 2020). This approach has the specificity to include explicit representations of key tissue types for water and solute transport, such as the xylem, phloem or aerenchyma (Couvreur *et al.* 2021).

Although the basic equation (3.5) appears rather simple, many different physiological factors affect the parameter values of σ and K. Moreover, these parameters may actually be variables that change over time, like $\kappa_{soil}(\theta)$ in equation (3.2). At the organ scale, the radial water transport across root tissues can change with root age (Vetterlein and Doussan 2016). Root growth creates a gradient in age along the root axis, with increasing formation of apoplastic barriers (Steudle and Peterson 1998), the initiation of secondary growth (for eudicot species; Gambetta *et al.* 2013) and the decreases in the expression and activity of aquaporins (Gambetta *et al.* 2013; Gambetta *et al.* 2017) at the older, proximal part. At a larger scale, the root system architecture is composed of individual roots with heterogeneous anatomical (e.g. stele diameter; Passot *et al.* 2016), physiological (e.g. aquaporin expression; Knipfer *et al.* 2011) and morphological (e.g. diameter; Rewald *et al.* 2011) functions and characteristics in different branching orders and root types (Hishi 2007; Passot *et al.* 2016; Saint Cast *et al.* 2020; Watanabe *et al.* 2020). These facts lead to the assumption that each root order or type may have different radial hydraulic conductivity. Therefore, the functional roles of these roots in water uptake may be different from each other, although few studies have focused on the heterorhizy from the aspect of root hydraulics (Watanabe *et al.* 2020). Alternatively, the exogenous environments (i.e. the climate, the soil, management practice, circadian rhythm) can influence the transport of water throughout the root (Caldeira *et al.* 2014; Tardieu *et al.* 2015). Indeed, the changing root properties are not only linked to the root age, the root order or the root type, but its intensity varies with root environment, particularly water availability (Lobet *et al.* 2014). For example, in drought-stressed rice or grapevine, suberization of the endodermis increased (Henry *et al.* 2012; Cuneo *et al.* 2021).

Far from being a temporal gradient of 'better models' but rather a diverse palette, each of the cited approaches currently has a niche determined by the compromise between its specificity and simplicity. On the one hand, in applications at the plant scale and beyond, radial water transport across root tissues is generally considered as driven by pressure gradients across a single hydraulic conductance, as already done by van den Honert (1948). Examples of this implementation comprise newly implemented plant hydraulic modules in TBMs (Bisht and Riley 2019; Kennedy *et al.* 2019; Sulis *et al.* 2019; Agee *et al.* 2021) but also recent FSPMs (Roose and Fowler 2004; Javaux *et al.* 2008; Postma *et al.* 2017; Bouda *et al.* 2018). An enrichment to this single hydraulic conductance model accounted for the osmotic potential difference between soil and xylem water, assuming that root tissues act like a semipermeable 'big membrane' analogous to an osmometer (Kramer and Boyer 1995), and transposed equation (3.5) to the root segment scale. On the other hand, applications including the study of tissue-specific water channels (Ding *et al.* 2020), the radial pathways of water tracers (Zarebanadkouki *et al.* 2019) or solute convection–diffusion and active transport (Foster and Miklavcic 2020) require the use of more detailed models accounting for the relevant processes and levels of granularity.

3.3 Water transport in the xylem

Transport of water and therein dissolved nutrients from roots to leaves is the major function of xylem. The main structural unit, present in all vascular plants is the xylem conduit, also called the tracheary element. Mature xylem conduits are dead cell wall skeletons and form a pipe-like structure without obstacles of cell membranes and protoplasts, thus providing high xylem hydraulic conductance K_{xylem} (Fig. 4). The length of individual xylem conduits ranges from several mm up to several m, with diameters between 5 μm in conifer needles and 500 μm in tropical lianas (Hacke and Sperry 2001; Sperry *et al.* 2006). Two xylem conduit types exist: tracheids and vessel elements. Tracheids are evolutionary older, and originate from individual cells. Vessel elements are interconnected to form a chain of cells (called vessels) where connecting end-walls are partially or completely replaced by perforation plates (Venturas *et al.* 2017). Both conduit types are connected to their neighbour conduits through large circular bordered pits (Fig. 4). Pit-pairs of adjacent cells are precisely aligned with pit membrane between them, comprised of modified primary walls and intervening middle lamella of neighbouring cells (Myburg *et al.* 2013). Although reducing hydraulic conductance, pit membranes play a crucial role in water transport, functioning as capillary safety valves.

As explained by the cohesion-tension theory (H. H. Dixon and Joly 1895; Venturas *et al.* 2017), water is pulled upwards from the roots to the leaves through the conduits formed by the xylem cells. Because the xylem conduits are dead cell wall skeletons, osmotic gradients do not play a role in xylem water transport. The xylem transport equation thus equals equation (3.5) with $\sigma = 0$. Moreover, because the concentration of solutes in xylem sap is generally low, the contribution of the osmotic component Ψ^{π} to the total water potential Ψ is often neglected (Nobel 1983; H. G. Jones 2015).

The hydraulic conductance of the xylem (K_{xylem}) can theoretically be approximated by the Hagen–Poiseuille equation for laminar flow in cylindrical pipes:

$$K_{xylem,i} = \frac{\pi \cdot r^4}{8 \cdot L \cdot \eta}, \tag{3.6a}$$

$$K_{xylem} = \sum_{i=1}^{n} K_{xylem,i}, \tag{3.6b}$$

where $K_{xylem,i}$ is the hydraulic conductance of xylem conduit i [m^3 MPa^{-1} s^{-1}], r is the xylem conduit radius (assumed to be a cylinder) [m], L the path length between the sites [m], η the dynamic viscosity of the xylem sap [MPa s] and n is the number of conduits in a cross-section of the xylem. Consequently, the mean xylem conduit radius as well as the number of xylem conduits are major determinants for total xylem hydraulic conductance. However, calculations based on this

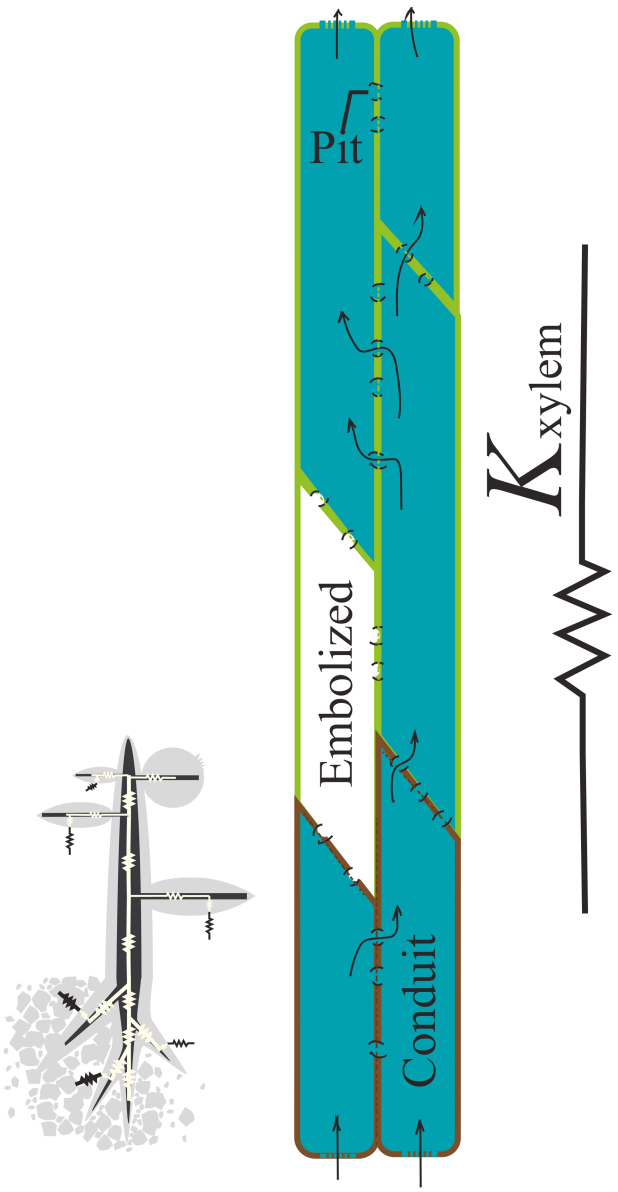

Figure 4. Scheme of water flow inside the xylem, from the roots to the leaf veins, where K_{xylem} is the xylem hydraulic conductance. Conduits in the xylem represent both tracheids and vessels and are connected to each other through pits. The embolized conduit (i=1) is no longer conductive, and forces the water flow to take an alternative path. Conduits i refer to parallel conduits as defined in equation (3.6). The dark region in the small image on the left indicates the location of the xylem in the SPAC.

approach always lead to overestimation of the actual hydraulic conductance, because a substantial part of the water transport occurs in the cell wall matrix, which has much smaller conduit radii, and because the effect of border pits or perforation plates is neglected (Martre *et al.* 2000) (Fig. 4). Water transport through pits has been modelled by means of computational fluid dynamics by Schulte (2012). Their 3D geometric models were based on scanning electron microscopy images. Such models provide a detailed insight in water flow mechanisms at the microscale.

The structure of xylem vasculature varies across species and changes with age. In conifers, vessel elements and fibres are completely absent from xylem. Conifer wood is 95 % tracheids by volume with a small amount of parenchyma present (Venturas *et al.* 2017). Tracheids are here, therefore, responsible for most of the functionality provided by xylem. Angiosperms, however, contain all types of cells: vessel elements, tracheids, fibres and parenchyma cells. Steppe and Lemeur (2007) demonstrated the effect of differing anatomical traits on the hydraulic parameters in their water transport model. But even in grasses, Martre and Durand (2001) and Martre *et al.* (2000) showed that developmental shifts from protoxylem to metaxylem in the leaf growth zone have major impacts on leaf hydraulic conductance.

Under specific conditions, xylem conduits may fill with air (i.e. cavitation), causing a phenomenon called embolism. In this situation, the passage of the water is blocked by the air bubble, and the conduit is no longer conductive (Fig. 4). The major driver for embolism is low hydrostatic water potential (e.g. during drought; Holbrook and Zwieniecki 1999), but also freeze-thaw cycles (Sperry and Sullivan 1992), leaf drop and herbivore activity can induce embolisms. For detailed insights in the mechanisms at play, we refer to Schenk *et al.* (2015) and Venturas *et al.* (2017). If multiple conduits are blocked by embolisms, the hydraulic conductance of the xylem can be substantially reduced. Mathematically, the resistance to xylem embolism is typically assessed by the vulnerability-to-cavitation curve (VC) which represents hydraulic conductivity as a function of xylem water potential (Sperry and Tyree 1988; Cochard *et al.* 2013). Alternatively, the VC can be used to quantify the percentage loss of conductance (*PLC*) as a function of xylem water potential (Fig. 5). Usually, *PLC* curves are modelled with an exponential or sigmoidal equation (Pammenter and Van der Willigen 1998) such as:

$$PLC = \frac{100}{\left(1 + e^{a(\Psi - \Psi_{50})}\right)} \tag{3.7}$$

These curves tend to be species-specific and provide derived parameters (Ψ_{12}, Ψ_{50}, Ψ_{80}: Ψ at *PLC* 12 %, 50 % and 88 %, respectively) to compare vulnerability among species (Choat *et al.* 2012). Hydraulic safety margins within which many plants operate are relatively narrow, with plants being resistant to embolism at pressures ranging from −0.1 MPa down to approximately −10 MPa (Jacobsen *et al.* 2007; Choat *et al.* 2012; Venturas *et al.* 2016). These functions can be used to rescale the hydraulic conductivity in equation (2.7) (Sperry *et al.* 2016).

3.4 Extra-xylary leaf water transport (K_{ox})

The last two decades, many studies have highlighted the importance of leaves in the whole-plant hydraulic pathway and have recently been reviewed by Scoffoni and Sack (2017). For example, under well-watered conditions, leaves account for at least 30 % of the hydraulic resistance within plants (Sack and Holbrook 2006). This is remarkable, because in the total transpiration-driven pathway, the path length

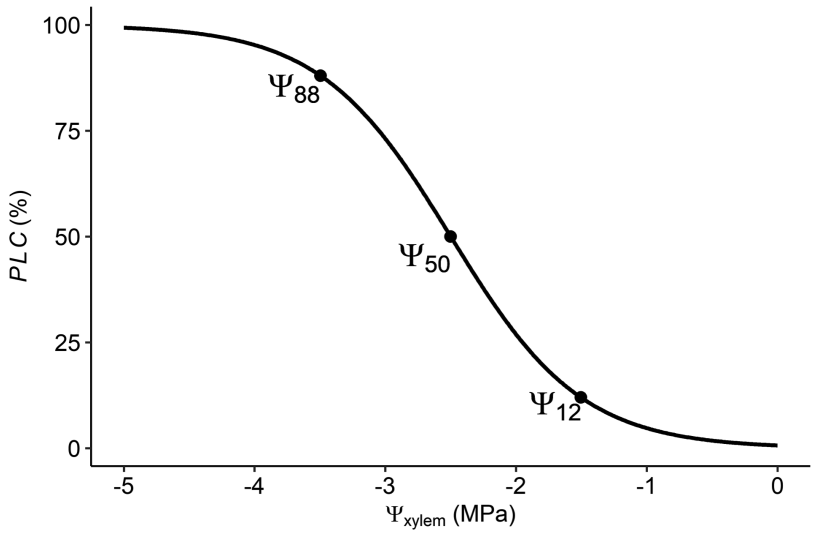

Figure 5. Percentage loss of conductance (*PLC*) as a function of xylem water potential Ψ_{xylem}, using equation (3.7), with $a = 2$ and $\Psi_{50} = -2.5$ MPa. Ψ_{12} and Ψ_{88} are the water potentials at which *PLC* equals 12 % and 88 %, respectively.

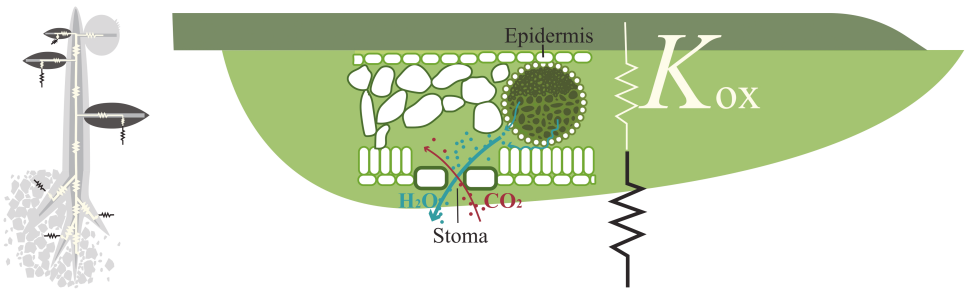

Figure 6. Scheme of water flow in the leaves, outside the xylem, from the leaf veins to the sites of evaporation, where K_{ox} is the outside-xylem hydraulic conductance. The dark region in the image on the left indicates the location of the leaves in the SPAC.

in leaves is only minor, except for most grasses. The total leaf resistance, and thus also the conductance (K_{leaf}) can be partitioned into a component associated to the leaf xylem, and a component outside the xylem (Fig. 6). The latter is often referred to as the outside-xylem conductance (K_{ox}), and can be as low as the leaf xylem conductance, although large variations occur across plant species (Scoffoni *et al.* 2016). Consequently, a substantial water potential gradient can exist from the xylem to the sites of evaporation (Martre *et al.* 2000; Martre and Durand 2001; Buckley 2015; Sack *et al.* 2015; Scoffoni *et al.* 2018). This gradient is of major importance for stomatal conductance regulation (Scoffoni *et al.* 2017).

A large number of studies have reported a decline in K_{leaf} with dehydration, having important repercussions on plant productivity, whole-plant water transportand drought responses (Scoffoni and Sack 2017). Similar to xylem vulnerability to cavitation (see Section 3.3), K_{leaf} can be expressed as a function of leaf water potential via the sigmoid *PLC* curve (Venturas *et al.* 2017).

Although many studies have pointed to xylem embolism as the main factor for reduced K_{leaf}, recent insights suggest that outside-xylem processes play the dominant role in the decline of K_{leaf} with dehydration (Scoffoni *et al.* 2017). Consequently, environmental drivers and plant anatomical and functional traits that determine K_{ox} have gained interest in recent years (Buckley 2015; Scoffoni *et al.* 2018; Earles *et al.* 2019). Anatomical leaf traits identified to impact K_{ox} are vein length per area, presence of bundle sheath extensions, mesophyll thickness and sponginess and presence of a suberized layer (Sack *et al.* 2015). Spatially explicit modelling work by Buckley (2015) demonstrated the large water potential drop between the leaf xylem and the sites of evaporation, under conditions of transpiration, mediated by low K_{ox}. Apart from the anatomical traits, Buckley (2015) identified additional impactful factors on K_{ox}. These authors dissected the apparent positive correlation between irradiance on K_{ox} into two factors: (i) effects of temperature gradients in the leaf on the conductivity in the gaseous phase, and (ii) effects of light on aquaporin functionality. These effects can additionally explain the variable hydraulic conductance observed experimentally (Cochard *et al.* 2007; Scoffoni *et al.* 2018). Explicit modelling of the outside-xylem water flow in leaves provides an opportunity to better understand and predict stomatal responses, especially under water-limited conditions (Scoffoni *et al.* 2017; Earles *et al.* 2019).

3.5 Models for the entire transpiration pathway

Models that describe the flow of water along the transpiration pathway were the earliest implementations of water potential in plant models. In this respect, the work of van den Honert (1948) was a milestone, as he connected four different parts of the transpiration stream by using an electric analogon: (i) living root cells, (ii) xylem, (iii) living leaf cells, (iv) gaseous phase in the leaf and the boundary layer. This idea was based on earlier work of Gradmann (1928), who suggested that any transport process where the velocity is proportional to a potential difference (water flow and diffusion) can be modelled using Ohm's law. As such, Hagen–Poiseuille's law, Darcy's law and Ohm's law, all used by modellers of water flow in soils and plants, are all closely related to the basic equation (2.7). The connection of t nodes j from as done by van den Honert (1948) corresponds to an electric circuit where resistances are connected in series. As such, the total resistance of the system R_{tot} equals the sum of all resistances:

$$R_{tot} = \sum_{j=1}^{t} R_j \tag{3.8a}$$

$$\frac{1}{K_{tot}} = \sum_{j=1}^{t} \frac{1}{K_j} \tag{3.8b}$$

$$= \frac{1}{K_{soil}} + \frac{1}{K_{plant}} \tag{3.8c}$$

$$= \frac{1}{K_{soil}} + \frac{1}{K_{root}} + \frac{1}{K_{xylem}} + \frac{1}{K_{ox}} \tag{3.8d}$$

Cowan (1965) complemented the approach of van den Honert by adding the soil as three additional compartments: (i) the sub-soil, (ii) the top-soil (i.e. the plant rooting zone) and (iii) the soil in direct vicinity of roots (rhizosphere). The work of Cowan (1965) and van den Honert (1948), essentially comes down to a series connection of (simplifications of) the water flow processes described in Sections 3.1–3.4. In the study of Cowan (1965), a capacitor was added in the model to cope with non-steady state, but only in the bulk soil compartments. In a comprehensive study, Hunt 1991 extended the concepts of Cowan by adding capacitors in the plant compartments (Fig. 7). They demonstrated that capacitance is required to properly simulate diel variations in water uptake and plant water potential, although steady-state models perform satisfactorily for simulations of daily or seasonal water uptake.

The recent model SurEau.c (Cochard *et al.* 2021) also describes the complete transpiration-driven water flow from the soil to the atmosphere for trees. However, in this model, the xylem pathway has been subdivided in multiple separate connected nodes, representing connected organ types: roots (three levels), trunk, branch and leaf. In each of these organ types, a symplastic node is connected to the xylem node (apoplast). Water transport between all connected nodes is described by a resistor and capacitor, enabling the model to simulate non-steady-state water transport. Recent implementations of 3D models include the entire transpiration pathway for a static plant architecture (Dauzat *et al.* 2001; da Silva *et al.* 2011; Albasha *et al.* 2019; Zhou *et al.* 2020), but also for dynamically growing plants (Coussement *et al.* 2018; Coussement *et al.* 2020). In these models the 3D architecture was used to simulate transpiration at the leaf level, based on spatially resolved light interception using complex raytracer (Henke and Buck-Sorlin 2017) or radiosity light models (Chelle and Andrieu 1998). However, only the CPlantBox model (Zhou *et al.* 2020) has a spatially explicit representation of the root system for modelling plant water uptake in three dimensions. Nevertheless, these 3D models introduce a conductance (or resistance) between all nodes, typically according to equation (2.8), taking into account the path length between the nodes and the average xylem cross-section (da Silva *et al.* 2011; Nikinmaa *et al.* 2014; Coussement *et al.* 2018). These nodes can represent internodes, leaves or fruits, and nodes can be connected to multiple other nodes (Dauzat *et al.* 2001). Figure 1 gives an overview on how conductances can be arranged in a plant-like structure.

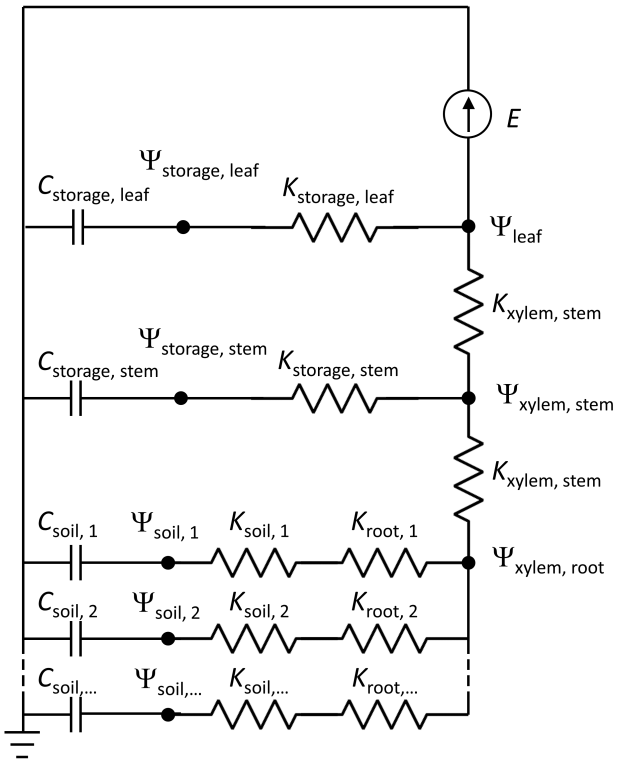

Figure 7. Schematic overview of the hydraulic model by Hunt *et al.* (1991), connecting multiple compartments of the SPAC as an electrical analogon. *C* stands for capacitance, *K* for conductance, Ψ for water potential and *E* for transpiration flux. The subscripts refer to the location in the SPAC (soil, root, stem, leaf), the plant tissue (xylem or storage tissue) and the soil/root layer (1, 2, ...).

Although there has clearly been an evolution towards more spatial resolution in modelling the water transport pathway, very simplified representations still exist and remain useful for studies at a higher spatial (e.g. Eller *et al.* 2020) or conceptual (e.g. Tuzet *et al.* 2003) scale. In its simplest form, modelling water transport from the roots to the leaves can be approximated by a single 1D pipe with a pressure

difference between the soil and leaf ends and a conductivity value K_{plant} (Martinez-Vilalta *et al.* 2002). In these models, the leaves of the plant are approximated by one 'big leaf' and the architecture of the plant is omitted.

4. PHLOEM WATER TRANSPORT

In addition to the xylem, which conducts the upward water flow associated to the transpiration stream (Section 3), phloem is the vascular tissue that facilitates long-distance transport of water and dissolved ions, hormones, sugars and amino acids. Because of their proximity in the vascular bundle, xylem and phloem functioning is closely connected (Fig. 8). However, while water in the xylem is generally under tension, and consequently has a negative hydrostatic pressure Ψ^p, the phloem operates under a positive Ψ^p. According to the Münch (1930) hypothesis, this positive pressure is generated by the loading of soluble photoassimilates (generally sucrose) and amino acids in the leaf phloem (i.e. collection phloem), which locally reduces the osmotic potential Ψ^π and attracts water from surrounding tissues like the xylem, thus generating an increase in the hydrostatic pressure Ψ^p (i.e. turgor pressure). At the sinks, the release phloem (i.e. growing tissues, roots, storage organs, fruits, etc.) unloads solutes, thereby increasing the osmotic potential, allowing water to flow out of the phloem and reducing the hydrostatic pressure. Consequently, the loading and unloading of soluble sugars and amino acids generates the pressure gradient for phloem flow (Stroock *et al.* 2014).

Similar to the xylem, the phloem has specific transport cell types, called sieve elements. Because these sieve elements are axially connected to each other by sieve plates, no semipermeable membranes are crossed along the path, and water transport in the phloem is only driven by the hydrostatic potential gradient ($\sigma = 0$ in equation (3.4)). Nevertheless, much is yet to be elucidated, as measured hydrostatic pressure gradients between source and sink are not reconcilable with the hydraulic resistance along the path, especially in large trees (Minchin and Lacointe 2017). Recent reviews discuss the current understanding of the nature and mechanisms of water and solute transport in the phloem for a plant science audience (van Bel 2003; De Schepper *et al.* 2013; Jensen 2018), as well as for physicists (Stroock *et al.* 2014), but in the current section we focus on the modelling attempts.

Based on the Münch (1930) hypothesis, multiple phloem transport models have been developed, differing mainly in spatial resolution and phloem anatomical complexity. Thompson and Holbrook (2003) provide an overview of the evolution of the phloem transport models that provide a spatially and temporally continuous solution, making use of partial differential equations. They identified several key studies in this area (e.g. Christy and Ferrier 1973; Ferrier *et al.* 1975; Smith *et al.* 1980) and highlighted the low availability of computational power as a major limitation in the further development of this type of models. Alternatively, some models simulated phloem water and solute transport between a limited number of discrete compartments, instead of throughout a spatial continuum (Thornley and Johnson 1990; Dewar 1993; Minchin *et al.* 1993; Sheehy *et al.* 1995). These studies have been used to explain carbohydrate allocation between sources and sinks in simple plant models, and basically function independent of the xylem. Daudet *et al.* (2002) were the first to connect phloem and xylem flow, an approach adopted by most later models for phloem transport (Hölttä *et al.* 2006, 2009; Lacointe and Minchin 2008; De Schepper and Steppe 2010). In their landmark study, Lacointe and Minchin (2008) harnessed the ever-increasing availability of computing resources to extend the work of Daudet *et al.* (2002) for application in more complex branched structures, connecting multiple sinks and sources, and including lateral leakage and retrieval mechanisms (Minchin and Lacointe 2017). Recently, a version of this model was included in the (static) root–shoot FSPM CPlantBox (Zhou *et al.* 2020).

Analytical solutions to the spatially continuous approaches have been proposed, but are limited to steady-state phloem water flow (Cabrita *et al.* 2013; Hall and Minchin 2013). Whether the spatial gradients are addressed in a continuous form or using discrete compartments, all models use (a variation of) the Hagen–Poiseuille concept for viscous flow (equation (3.6)). Discrete compartment models have been more popular in recent years, thanks to their computational efficiency, and confirmed correspondence with the spatially continuous models (Minchin and Lacointe 2017). Some of these discrete compartment models have simplified the Hagen–Poiseuille equation and can be seen as transport-resistance models following the basic equation (2.7) (Lacointe and Minchin 2008; De Schepper and Steppe 2010; Zhou *et al.* 2020).

On the other hand, some studies (Thompson and Holbrook 2003; Jensen *et al.* 2012; Cabrita *et al.* 2013; Jensen 2018) have derived more complex models for phloem flow to explicitly take the impact of sieve plates on the hydraulic conductance in the phloem into account. As such, these models have aided to elucidate how phloem anatomy impacts the hydraulic conductance, and concluded that sieve plates account for about half of the hydraulic resistance in the phloem. Such models and their physically based parameters allow to highlight potentially relevant traits for carbon allocation efficiency.

5. PHYSIOLOGICAL LINKS TO WATER POTENTIAL

In Sections 3 and 4, we reviewed how hydraulic models simulate water transport between plant organs along the major hydraulic pathways. However, other water transport paths (e.g. between epidermal and guard cells, or towards growing tissues) mediate important physiological processes like stomatal conductance and cell elongation. In the next sections we focus on the models that link water potential and these physiological processes.

5.1 Stomatal conductance

Regulation of stomatal conductance is a complex process that is affected by microclimate (light and vapour pressure deficit), leaf CO_2 concentration, plant hormones, leaf water potential and soil water potential (see reviews by Damour *et al.* 2010; Buckley 2017). Stomatal conductance models can be roughly classified in three types: process-based, optimality-based and (semi-) empirical.

Process-based models aim to describe stomatal behaviour based on the underlying detailed passive (related to the hydraulic connection between epidermal and guard cells), and active (related to the production of hormones such as leaf endogenous abscisic acid) mechanisms (Brodribb and McAdam 2017). Both active and passive

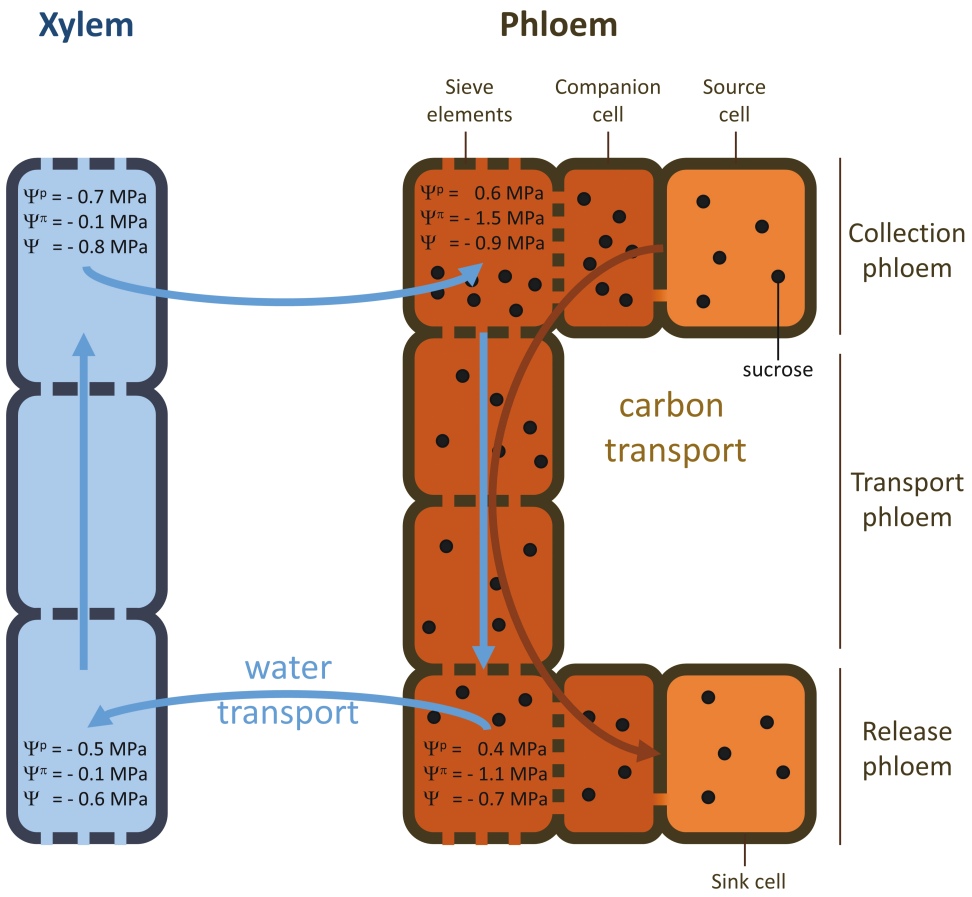

Figure 8. Scheme of the xylem–phloem interaction, and the Münch (1930) mechanism exemplified by hypothetical (yet realistic) gradients in hydrostatic (Ψ^P), osmotic (Ψ^π) and total water potential (Ψ).

stomatal responses are strongly connected to leaf water potential (Buckley 2017). Complex process-based stomatal conductance models (e.g. the models of Cooke *et al.* 1976; Dewar 2002; Buckley *et al.* 2003; Franks 2004; Hills *et al.* 2012) are invaluable for studying the mechanisms of stomatal behaviour and kinetics in response to light, CO_2 and water stress. However, these process-based models include many biophysical parameters that can be very difficult to measure, and are, therefore, currently under-exploited in plant and ecosystem models (Buckley 2017). Therefore, efforts have been made to simplify these process-based models for broader use, yielding fewer parameters that need to be estimated, while retaining clear connections to the detailed processes (Buckley *et al.* 2012; Diaz-Espejo *et al.* 2012; Rodriguez-Dominguez *et al.* 2016).

Optimality-based models start from the hypothesis that, due to evolutionary drivers, plant species have optimized the trade-off between carbon gain and water loss (Cowan *et al.* 1977). These models are built on the assumption that stomatal opening is modulated such that the marginal water use efficiency is constant for a relatively short period of time (Cowan *et al.* 1977; Hari *et al.* 1986; Wolf *et al.* 2016):

$$\lambda = \frac{\delta A_n / \delta g_s}{\delta E / \delta g_s}, \tag{5.1}$$

which implies that the profit of an increased net photosynthesis rate (δA_n; [mol CO_2 m^{-2} s^{-1}]) in response to a small increase in stomatal conductance (δg_s; [m s^{-1}]) equals the corresponding increase in evaporative water loss (δE; [m s^{-1}]) multiplied by the carbon cost of water (λ; [mol CO_2 m^{-3} H_2O]). The models built on this hypothesis have demonstrated successful predictions of stomatal responses to most environmental and photosynthetic variables. However, proper interpretation of λ remains difficult, especially because the value of λ changes with varying soil moisture availability varies or when plants are competing for water (Wolf *et al.* 2016; Buckley 2017; Sperry *et al.* 2017).

To overcome this limitation under variable or reduced water availability, the introduction of a carbon cost function, associated with repairing hydraulic conductance originating from low xylem water potential, has been proposed (Wolf *et al.* 2016; Sperry *et al.* 2017). In these models, stomatal conductance is predicted from a carbon maximization optimization, rather than from the original marginal water use efficiency. In these approaches, both the carbon cost function and E were defined as a function of leaf water potential. Recently, Eller *et al.* (2020) and Sabot *et al.* (2020) have presented slightly different versions of these hydraulically based stomatal optimization models in the land surface models JULES and CABLE. These recent

developments highlight the improved performance of models when including hydraulics, especially under drought conditions, based on flux tower and hydraulic trait data sets. The review by Mencuccini *et al.* (2019) provides a clear overview of optimal-based model types combining stomatal behaviour and hydraulic functioning.

Semi-empirical models describe the response of stomatal conductance to environmental and internal plant variables, based on empirically derived relationships. The most commonly used models belong to the so-called Ball–Berry–Leuning (BBL) 'family', and build on the equations developed by Ball *et al.* (1987) and Leuning (1995):

$$g_s = g_{s,0} + g_{s,1}\frac{A_n}{([C_a]-\Gamma)\left[1+\left(\frac{\delta e}{d_1}\right)\right]}, \tag{5.2}$$

where $g_{s,0}$ is the minimum stomatal conductance [m s^{-1}], δe is the vapour pressure deficit [kPa], $[C_a]$ is CO_2 concentration at the leaf surface [ppm], Γ is the CO_2 compensation point [ppm] and $g_{s,1}$ [m^3 ppm mol^{-1}] and d_1 [kPa^{-1}] are empirical coefficients. More recent publications have indicated the convergence of these empirical models with the optimality-based approach under certain conditions (Medlyn *et al.* 2011; Wolf *et al.* 2016; Sperry *et al.* 2017; Duursma *et al.* 2019). Empirical leaf-level models of stomatal conductance in plant and ecosystem models perform satisfactorily under well-watered conditions, but show substantial inconsistencies under drought stress or variable watering conditions (Tuzet *et al.* 2003; Buckley 2005; Damour *et al.* 2010; Anderegg *et al.* 2017). This leads to a large uncertainty in transpiration predictions from plant, crop and ecosystem models (Carminati and Javaux 2020). As an adaptation to the BBL models, Nikolov *et al.* (1995) and Tuzet *et al.* (2003) suggested including a sigmoid response function to leaf water potential as a multiplication factor to the second term of the BBL model:

$$f(\Psi_{leaf}) = \frac{1}{1+\left(\frac{\Psi_{leaf}}{\Psi_{1/2}}\right)^p}, \tag{5.3a}$$

$$f(\Psi_{leaf}) = \frac{1+e^{s_1\Psi_0}}{1+e^{s_1(\Psi_0-\Psi_{leaf})}}, \tag{5.3b}$$

where the coefficients $\Psi_{1/2}$ [MPa] and p [dimensionless] (Nikolov *et al.* 1995), and s_1 [MPa^{-1}] and Ψ_0 [MPa] (Tuzet *et al.* 2003) describe the sensitivity to the leaf water potential Ψ_{leaf} [MPa].

Despite the widespread use of BBL models, other (even earlier) empirical models already included the effect of leaf water potential. A first empirical model that included dependency on leaf water potential was presented by Jarvis *et al.* (1976). This was a response-function approach, where stomatal conductance (g_s) was related to photosynthetically active radiation (Q_p; [μmol m^{-2} s^{-1}]), leaf temperature (T_{leaf}; [K]), vapour pressure deficit (δe; [kPa]), leaf water potential (Ψ_{leaf}; [MPa]) and ambient CO_2 concentration ($[C_a]$; [ppm]) in a multiplicative manner:

$$g_s = g_{s,max}\cdot f_1(Q_p)\cdot f_2(T_{leaf})\cdot f_3(\delta e)\cdot f_4(\Psi_{leaf})\cdot f_5([C_a]), \tag{5.4}$$

where $g_{s,max}$ [m s^{-1}] is the maximum stomatal conductance and each of the response functions f results in a value between 0 and 1. The response function for Ψ_{leaf} was presented as a negative exponential relation:

$$f_4(\Psi_{leaf}) = 1 - e^{-s_2(\Psi_{leaf}-\Psi_{min})}, \tag{5.5}$$

where s_2 is a curvature parameter and Ψ_{min} the water potential at which the response function becomes zero. Dauzat *et al.* (2001) included a similar approach in their plant model of *Coffea arabica*, but omitted the response function for $[C_a]$ and modified the response function for Ψ_{leaf}:

$$f_4(\Psi_{leaf}) = \frac{\Psi_{leaf}-\Psi_{min}}{\Psi_{max}-\Psi_{min}} \tag{5.6}$$

Alternatively, leaf water potential has been used as an explanatory variable for the sensitivity of stomatal conductance to abscisic acid concentration [ABA] (Tardieu and Davies 1993; Tardieu *et al.* 2015):

$$g_s = g_{s,0} + g_{s,1}\cdot e^{\beta\cdot[ABA]\cdot e^{s_3\cdot\Psi_{leaf}}}, \tag{5.7}$$

where $g_{s,0}+g_{s,1}$ is the maximum stomatal conductance [m s^{-1}], β is the sensitivity to abscisic acid concentration and s_3 [MPa^{-1}] reflects the stomatal sensitivity to Ψ_{leaf}.

Anderegg *et al.* (2017) compared the performance of four stomatal conductance models on under a wide range of conditions: the empirical model of Tuzet *et al.* (2003) and the optimality-based model of Wolf *et al.* (2016), both including a dependency on leaf water potential, and the optimal–empirical model of Medlyn *et al.* (2011) and the empirical model of Leuning (1995), both without a dependency on leaf water potential (Anderegg *et al.* 2017). This comparison demonstrated a better performance of the models that include water potential, and as such underpinned the importance of including the stomatal sensitivity to declining leaf water potential in plant and ecosystem models during drought conditions.

Furthermore, including the dependency on leaf water potential provides identification of a continuum of stomatal strategies during drought stress across and within species (Tardieu and Davies 1993; Tardieu *et al.* 2015). As such, the parameters $g_{s,0}$, $g_{s,1}$, p, s_1, s_2, s_3, Ψ_0, Ψ_{min} and Ψ_{max} (Jarvis *et al.* 1976; Tardieu and Davies 1993; Dauzat *et al.* 2001; Tuzet *et al.* 2003) could define the position of a species or genotype in this continuum, but also allow deeper interpretation, beyond the aniso/isohydric paradigm (Hochberg *et al.* 2018). Additionally, connecting hydraulics and stomatal conductance allows to study the potential 'hydraulic efficiency–hydraulic safety' trade-off of different plant species, in terms of drought resistance for vegetations and for agricultural production (Holloway-Phillips and Brodribb 2011; Martin-StPaul *et al.* 2017; Scoffoni and Sack 2017; Cardoso *et al.* 2018; Deans *et al.* 2020; Xiong and Nadal 2020). Robust models of stomatal conductance including leaf water potential are thus greatly welcomed to predict plant–atmosphere interactions in a changing climate but also to integrate new knowledge in physiology and ecological theory (Buckley 2017).

5.2 Cell, organ and plant growth

As plant tissues contain a large proportion of water, the dimensions and mass of plant organs are largely determined by the water accumulation,

which can be seen as the sum of incoming and outgoing water flows (Hilty *et al.* 2021). Since water potential drives water transport, the link between water potential and organ growth is strong. In modelling work, several approaches have been made to connect water potential to growth, be it through empirical relations, or through more mechanistic links that explicitly model water accumulation and involve turgor pressure.

Dewar (1993) developed an empirical root–shoot partitioning model, where the relative growth rate (RGR) of both the root and shoot compartment depend on the concentrations of carbon and nitrogen and on the xylem water potential in a multiplicative model:

$$\frac{1}{W}\cdot\frac{dW}{dt} = k_g\cdot[C]\cdot[N]\cdot max\left(1-\frac{\Psi}{\Psi_{crit}}\right), \tag{5.8}$$

where W is the dry matter mass per unit ground area [kg m^{-2}], k_g is a growth coefficient [s^{-1}], $[C]$ and $[N]$ are the carbon and nitrogen substrate concentrations [dimensionless], respectively, and Ψ_{crit} is a critical water potential for growth. Similarly, but on an architecturally more complex scale, da Silva *et al.* (2011) multiplied the RGR of each organ in the L-Peach FSPM with a linear function of the prevailing local water potential.

At the organ level, models of leaf elongation rate (LER) are of particular interest in grasses, as these predominantly grow in one dimension. Tardieu *et al.* (2015) developed an empirical model for LER in maize based on a genotype-specific maximum rate a_{LER} [m s^{-1}], a sensitivity c_{LER} [MPa^{-1}] to xylem water potential and a small dependency on xylem abscisic acid concentration a_{ABA} [m s^{-1}]:

$$\text{LER} = max(a_{LER} + min(a_{ABA}\cdot log(\,[\,\text{ABA}\,]\,),0)\cdot(1+c_{LER}\cdot\Psi_{xylem}),0) \tag{5.9}$$

More mechanistic approaches for modelling growth, mostly rely on the biophysical model for irreversible (plastic) cell growth, defined by Lockhart (1965) for one-dimensional growth, and adapted by Ray *et al.* (1972) for volumetric growth:

$$\frac{1}{V}\cdot\left(\frac{dV}{dt}\right)_{pl} = \phi\cdot max((\Psi^p - Y),0) \tag{5.10}$$

Here, V is the cell volume [m^3], the subscript 'pl' refers to 'plastic' growth, ϕ [MPa^{-1} s^{-1}] and Y [MPa] are parameters describing cell wall relaxation and yielding in response to the hydrostatic potential (i.e. turgor pressure) Ψ^p [MPa]. The parameter ϕ is generally named wall extensibility, and Y is the threshold turgor pressure above which no wall yielding occurs. Both parameters define the ability of the wall to grow: wall yielding ability increases with higher values for extensibility ϕ and lower values for threshold Y (Cosgrove 1993).

Many models of cell growth build on this relationship (Cosgrove 1993), but this concept has been expanded to models of organ growth. Arkebauer *et al.* (1995) used this equation to model leaf growth in maize, by summing cell growth of discrete cell volume classes. Daudet *et al.* (2002) conceptualized a fruit as a single cell and used equation (5.10) to model fruit growth as a part of their linked xylem–phloem model (see also Section 4).

Apart from the irreversible, plastic growth (equation (5.10)), also reversible, elastic changes in cell and organ volume take place (Ortega 1985). Moreover, modelling these elastic changes have been proven very insightful for studying plant responses to its environment (see, e.g., review De Swaef *et al.* 2015). To this end, several models have used Hook's law to link water potential to diel variations in stem xylem and phloem diameter (Perämäki *et al.* 2001; Zweifel *et al.* 2001; Sevanto *et al.* 2002, 2008; Hölttä *et al.* 2006; Steppe *et al.* 2015):

$$\frac{1}{V}\cdot\left(\frac{dV}{dt}\right)_{el} = \frac{1}{\varepsilon}\cdot\frac{d\Psi^p}{dt} \tag{5.11}$$

where ε is the volumetric elastic modulus [MPa], which is lower for more elastic materials. The assumption of Lockhart (1965) and Ray *et al.* (1972) of a constant pressure in the cell, thereby ignoring elastic effects, is thus not valid in dynamically growing plant cells and tissues. Ortega (1985) added an elastic term, based on Hook's law, to the Lockhart equation (equation (5.10)), resulting in an analogue to the viscoelastic Maxwell equation:

$$\begin{aligned}\tfrac{1}{V}\cdot\tfrac{dV}{dt} &= \tfrac{1}{V}\cdot\left(\tfrac{dV}{dt}\right)_{pl} + \tfrac{1}{V}\cdot\left(\tfrac{dV}{dt}\right)_{el}\\ &= \phi\cdot max((\Psi^p - Y),0) + \tfrac{1}{\varepsilon}\cdot\tfrac{d\Psi^p}{dt}\end{aligned} \tag{5.12}$$

Like equation (5.10), this augmented growth equation (5.12) has initially been used to mathematically describe the growth of individual cells (Ortega 1985; Cosgrove 1993; Proseus *et al.* 1999), but proved also very useful and intuitive when applied to entire tissues. As such, based on equation (5.12) models have been developed that link turgor pressure to growth of all plant organ types: roots (Génard *et al.* 2001), woody stems (Génard *et al.* 2001; Steppe *et al.* 2006; De Schepper and Steppe 2010), fleshy fruits (Fishman and Génard 1998; Lescourret and Génard 2005; Lechaudel *et al.* 2007; H.-F. Liu *et al.* 2007), herbaceous stems (De Swaef and Steppe 2010; De Swaef *et al.* 2013) and leaves (Barillot *et al.* 2021; Coussement *et al.* 2021). These concepts have furthermore been included in models that simulate (vertical) water transport across organs (Steppe *et al.* 2006; De Schepper *et al.* 2010; De Swaef *et al.* 2013). More recently, this has been further refined at the individual organ scale (internode, leaf, fruit) in FSPMs, where the 3D organ dimensions and plant architecture are explicitly simulated and visualized, and cumulate to whole-plant growth dynamics (Coussement *et al.* 2018, 2020).

Although equation (5.12) has been applied for all plant organs and provides an elegant and mechanistic view on organ growth, there is still much to investigate on the elastic modulus ε, extensibility ϕ and threshold Y parameters, as these are probably not fixed values, but are likely to vary with cell/tissue age (Proseus *et al.* 1999), with internal turgor (Proseus and Boyer 2006) and hormone concentration (Cosgrove 1993, 2005).

To improve understanding of these biophysical properties, mechanistic models describing mechanical deformation of cells and tissues driven by turgor pressure and incorporating their actual 3D geometry have been developed (Abera *et al.* 2014a, b; Fanta et al. 2014; Diels *et al.* 2019). Because of the large number of cells in a plant organ, it is impossible to extend these models to the entire plant. In the multiscale modelling paradigm, microscale models are used to compute material properties of the macroscale (Aregawi *et al.* 2014). Such models allow, for example, to evaluate the effect of a change in cell wall elastic

modulus or plasma membrane permeability on water transport in the organ and plant growth.

6. DISCUSSIONS AND PERSPECTIVES

6.1 Water potential as a connector

As described above, water potential is a variable common to all sites in the SPAC. Consequently, it offers a means of communication between soil and plant scientists, and is often used in models connecting soil and root hydraulics (Javaux *et al.* 2013; Couvreur *et al.* 2014). Furthermore, many transpiration-driven water transport models already connect soil, root and plant xylem, in more or less architectural or physiological detail (see Section 3.5). Such a soil–rhizosphere–plant hydraulics model has recently demonstrated its value by elucidating the crucial role of rhizosphere hydraulics on plant water relations (Carminati and Javaux 2020). Water potential has thus primarily been used as a model variable for simulations of transpiration-driven water transport, thereby integrating the effects of both soil and atmosphere conditions, and as such, fulfilling its role as a robust quantitative estimator of plant water status (Steppe 2018).

From this water status perspective, the link between plant hydraulics and stomatal conductance is not far-fetched, as stomatal conductance is part of the transpiration pathway. In fact, mechanistic models of stomatal conductance have already highlighted the pivotal role of leaf water potential in stomatal functioning (Buckley 2017; Earles *et al.* 2019). Recent phloem water (and solute) transport models always operate in close connection to the transpiration pathway (mostly the xylem), and thus provide detailed insights in how plant water status and transport are intertwined with carbon allocation (Stroock *et al.* 2014; Minchin and Lacointe 2017). Through xylem and phloem transport modelling, water potential also enables connecting the root to the shoot, as recently demonstrated in the CPlantBox FSPM (Zhou *et al.* 2020). Via its effects on stomatal conductance (carbon assimilation) and phloem water transport (carbon and nitrogen allocation), plant water potential is indirectly associated to plant growth. Because water potential gradients drive the water transport towards growing tissues, there is an additional strong direct link (Martre and Durand 2001; Muller *et al.* 2011). A schematic overview of linked mechanisms with water potential implemented in models is given in Fig. 9. Obviously, water potential is not the only systemic variable that impacts plant functioning. Plants cannot survive without the uptake, assimilation and allocation of carbohydrates, amino acids, nutrients and hormones, which regulate functioning in all plant organs. Hence, as carbon is the building block for all organic compounds in plants, the current emphasis of plant and crop models on photosynthesis and carbon allocation remains justified. Nevertheless, these compounds generally operate in aqueous solution and are transported throughout the plant via water. Furthermore, because of their solubility in water, many nutrients and assimilates contribute to the osmotic potential, and are thus closely linked to water potential.

Recent reviews (Fatichi *et al.* 2016; Mencuccini *et al.* 2019) have highlighted that modelling plant hydraulics, with water potential as a central variable, has been applied successfully, albeit not widely, on all scales: from detailed mechanistic cell scale models of stomatal conductance and cell division and expansion (Buckley *et al.* 2003; Abera *et al.* 2014b), over functional–structural plant scale models (Coussement *et al.* 2020) to large ecosystem scale models (Anderegg and Venturas 2020). Recently, the hydraulically based ecosystem model TREES has been modified for a cotton crop (Wang *et al.* 2020), but implementations of plant hydraulics in widely used crop models are still absent (Parent and Tardieu 2014). Typically, crop models do include effects of both soil water availability and atmospheric conditions on transpiration rate and biomass accumulation. However, they do not capture interaction effects of both, because they do not explicitly include water transport processes in the soil and plant. Especially for plant and crop responses to drought, the role of water transport is crucial, and thus also deserves attention in crop models (Parent and Tardieu 2014; Wang *et al.* 2020). Furthermore, because this overall plant response is an integration of many interacting underlying physiological responses, a proper coordination of these interactions is a key challenge for crop models (Parent and Tardieu 2014). By including a hydraulic component in crop models, water potential may serve as the pivotal variable coordinating plant water status effects on multiple physiological mechanisms, and consequently shaping the whole-plant response, as visualized in Fig. 9. Apart from the aforementioned connections to stomatal conductance, phloem transport and organ growth, some models have already associated plant water potential to nitrogen uptake and fixation (Thornley and Johnson 1990; Dewar 1993; Thornley 1998; Y. Liu *et al.* 2011). For example, in the Hurley Pasture model (Thornley 1998), the factor taking into account soil water deficit is a function of root water potential, as this was suggested to be a more stable link between water stress and N fixation than soil water content. Furthermore, water potential could be included in (sub-)models dealing with plant development and phenology, because drought stress may substantially impact, e.g., early flowering and senescence (J. Jones *et al.* 2003) or tree cambial activity (Cabon *et al.* 2020).

6.2 Identifying phenotypic traits for drought tolerance

6.2.1 Models for dissecting phenotypic traits.

CSMs and FSPMs are both considered ecophysiological model types, because they capture the effects of dynamic environmental conditions on plant physiological mechanisms underpinning the integrated plant response and resulting phenotype. These models contain species- and genotype-specific parameters, which are theoretically invariable under a wide range of environmental conditions (Hammer *et al.* 2006; Yin and Struik 2010). Genotype-specific parameter sets are thus expected to have higher heritability than associated, directly observed phenotypic traits. Therefore, model-assisted phenotyping holds promise to speed up genetic progress, by linking genetics to model parameters instead of to complex integrative traits like yield. Furthermore, these ecophysiological models assist also to highlight promising (combinations of) phenotypic traits for targeted populations of environments (Martre *et al.* 2015; Cooper *et al.* 2021). However, successful applications of model-assisted phenotyping require sufficient representation of relevant physiological mechanisms in the model (Parent and Tardieu 2014). This is especially true for drought stress tolerance traits, because a specific trait can be beneficial for crop performance in specific drought conditions while the same trait can be undesirable in other drought stress scenarios (Tardieu 2012). In that perspective,

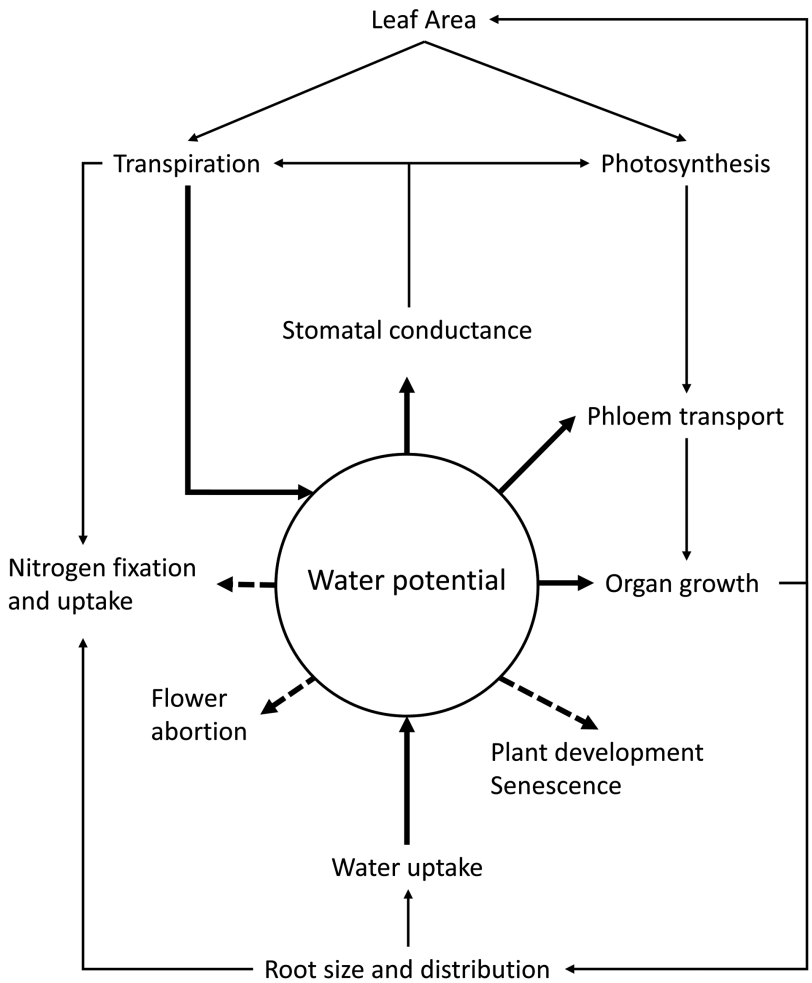

Figure 9. Water potential as a central variable connecting plant physiological processes. Thick arrows indicate direct links between water potential and processes. Full thick arrows identify links that have been included in current mechanistic plant models. Dashed arrows identify links that have been made empirically, but are as yet not often included in plant models. Thin arrows visualize links between processes to indicate indirect feedback effects on water potential.

traits associated to drought tolerance, listed in Table 1 of Tardieu (2012), should be dissected into its underlying interacting mechanisms. Models including soil–plant hydraulics, therefore, open up a whole new world of mechanisms and associated traits (Tardieu and Tuberosa 2010; Wang *et al.* 2020; López *et al.* 2021).

As an example, the trait associated to limiting transpiration rate at high evaporative demand (LTR trait) has received much attention as potentially beneficial for crop productivity in dry and warm environments, because it conserves water for a longer period in the growing season (Sinclair *et al.* 2017). This trait is the result of stomatal closure during midday, but Schoppach *et al.* (2013) showed that several plant hydraulic traits are associated with the LTR trait. Recently, the LTR trait has been implemented as a module into the APSIM NextGen model to investigate the impact of LTR on crop performance across multiple environments in Australia (Collins *et al.* 2021). Nevertheless, Devi and Reddy (2020) experimentally demonstrated that the parameter values associated with the LTR trait shift when soil moisture availability changes, potentially undermining the heritability of the trait. Recent soil–plant hydraulic modelling efforts have explained such responses by demonstrating the impact of rhizosphere hydraulic conductivity limitations associated with soil moisture content (Carminati and Javaux 2020). Including hydraulics in models thus allows to investigate how this LTR trait is impacted by soil moisture availability and how the trait can potentially be dissected into sub-traits. Both of these steps potentially enhance the heritability of this trait, but also the performance and interpretability of the model simulations.

6.2.2 Traits of interest and plasticity.

Making abstraction of the dynamic viscosity (η), equation (2.8) shows that hydraulic conductance is defined by the path length (L), the cross-sectional area perpendicular to the flow direction (A) and the permeability (k), which is an intrinsic characteristic of the medium. In Fig. 10, multiple morphological and physiological traits are summarized that impact the hydraulic conductance along the SPAC, through (at

least) one of these factors. All of these traits operate at the tissue level and drive local hydraulic functioning. However, at least as important is how these local traits are scaled to the entire plant, e.g. safeguarding the balance between supply and demand. Therefore, additional important trait examples relating to this balance are the total leaf area (cf. demand for water), root absorbing surface area (cf. supply of water) and ratios thereof (Christoffersen *et al.* 2016; Choat *et al.* 2018; López *et al.* 2021): leaf-to-sapwood area (for trees), root-to-shoot ratio and leaf-to fine-root absorbing surface area ratio.

Many of these traits can be implemented in various detail in plant and crop models as fixed parameters. However, virtually all of them tend to change with environmental conditions, and thus express plant plasticity, although the time scales may vary. An example of great interest is the xylem VC or the closely related *PLC* curve, where hydraulic conductivity is rescaled by a sigmoid or exponential response function to xylem water potential (equation (3.7)). This response function quantifies the impact of embolisms in the xylem conduits on hydraulic conductance, and variation in its parameters over species (e.g. Ψ_{50}) provides an interesting avenue to model ecosystem dynamics Anderegg 2015; Choat *et al.* 2018). Potentially, assessment of within-species genotypic differences in *PLC* may contribute to improving drought tolerance in crops (Wang *et al.* 2020).

Aquaporins are the plant's active regulation mechanism of hydraulic conductance, and their abundance has been shown to respond to transpiration and soil moisture (Vandeleur *et al.* 2009; Vandeleur *et al.* 2014), although responses of aquaporin expression can be completely opposite between species (North *et al.* 2004). From this perspective, the xylem water potential, which is also impacted by both transpiration rate and soil water availability, might be a suitable explanatory variable for hydraulic conductance variability attributed to aquaporin abundance (Chaumont and Tyerman 2014).

Traits associated to balancing plant water supply and demand may be mediated by water potential in a more indirect and complex way. For example, models that link water potential to organ growth show reduced leaf growth (and thus leaf area) as a plastic response to water deficits, thereby reducing (future) water demand (Arkebauer *et al.* 1995; Coussement *et al.* 2021). Furthermore, Dewar (1993) already demonstrated that a lower water potential as a result of increased transpiration or decreased soil water availability, increased the root-to-shoot ratio, using their water potential-driven conceptual model. Both examples show that the emergent properties of hydraulically mediated models enable capturing interesting plastic behaviour in response to drought.

Apart from the hydraulic traits discussed above and identified in Fig. 10, placing water potential central in a model as a coordinating variable opens opportunities to connect other, non-hydraulic traits and plastic responses. For example, the water potential-dependent function in the stomatal conductance model of Tuzet *et al.* (2003) allows to describe distinct stomatal sensitivity between species or genotypes using two parameters (equation (5.3b)). Figure 11 demonstrates how variations in hydricity between species or genotypes can be captured. The resulting parameter values for s_1 and Ψ_0 and may than serve as 'traits'. Furthermore, because the stomatal conductance model of Tuzet *et al.* (2003) is coupled to photosynthesis, this behaviour also captures short-term plasticity in terms of carbon assimilation. Such a model, linking plant hydraulics to stomatal conductance, can dissect overall stomatal conductance responses into hydraulic (K_{plant}) and stomatal conductance traits (s_1 and Ψ_0). This may be of great importance for interpreting plant phenotyping studies that use thermography for assessing drought tolerance (H. G. Jones 2015).

Chen *et al.* (2021) combine biophysical and biochemical modelling in their virtual fruit for tomato, which is connected to the stem through xylem and phloem water and solute fluxes, driven by water potential gradients (Génard *et al.* 2007). Via a global sensitivity analysis, Chen *et al.* (2021) demonstrate the importance of certain traits to improve tomato production and quality. The three most influential parameters for improving fresh yield were all biophysical in nature (the hydraulic conductance of the phloem (K_{phloem}), the phloem osmotic water potential caused by the solutes other than sugars and the fruit cell wall extensibility (ϕ)), whereas fruit quality was mostly sensitive to biochemical parameters. Consequently, their virtual fruit has demonstrated the potential uncoupling of the size–sweetness trade-off in fleshy fruit. In their hydraulic-based biophysical FSPM for soybean, Coussement *et al.* (2020) show how both hydraulic (e.g. hydraulic resistance) and non-hydraulic parameters (e.g. tissue extensibility) impact organ and plant dimensions under dynamic environmental conditions. Furthermore, they assessed the impact of modified air humidity and soil water potential as external drivers to demonstrate the model's ability to capture plastic growth responses associated to water availability. These models that embed water potential as a pivotal variable in association to other plant processes thus allow to study the impact of hydraulic traits on overall plant performance under a wide range of conditions, including drought.

6.3 Drowning in model complexity?

Models that include hydraulic features are thus very insightful, especially when the link is made with plant and organ growth. However, a potential pitfall with including hydraulics in models is that these models become overly complex. Therefore, they may be difficult to parameterize (Peng *et al.* 2020). Modellers should thus strive to design models 'as simple as possible, as complex as necessary', and backed by sufficient experimental data (He *et al.* 2017). Plant simulation models remain approximations of reality, and never include all possible mechanisms. Therefore, the mechanisms included in models (e.g. hydraulics) should match the research questions they address.

Tardieu *et al.* (2020) propose the terminology of 'meta-mechanisms' to explain that models operating at distinct scales of organization (from cell to crop) tend to have a similar complexity, because simplifications are proportional to the scale of organization. Such meta-mechanisms are, for example, response curves to environmental conditions. One concrete example is the temperature response curve for modelling plant development rate in crop models, where many underlying 'mechanisms' at the cell and tissue scale shape this integrative response. In their Figure 1, Tardieu *et al.* (2020) classify mechanisms associated with hydraulics in models at the organ scale. However, based on recent developments in FSPMs and ecosystem scale models, we would suggest that hydraulics have their place in models on all scales of organization, because hydraulics can be represented in different levels of complexity (Fatichi *et al.* 2016; Mencuccini *et al.* 2019). For example, the xylem vulnerability curves or percent loss

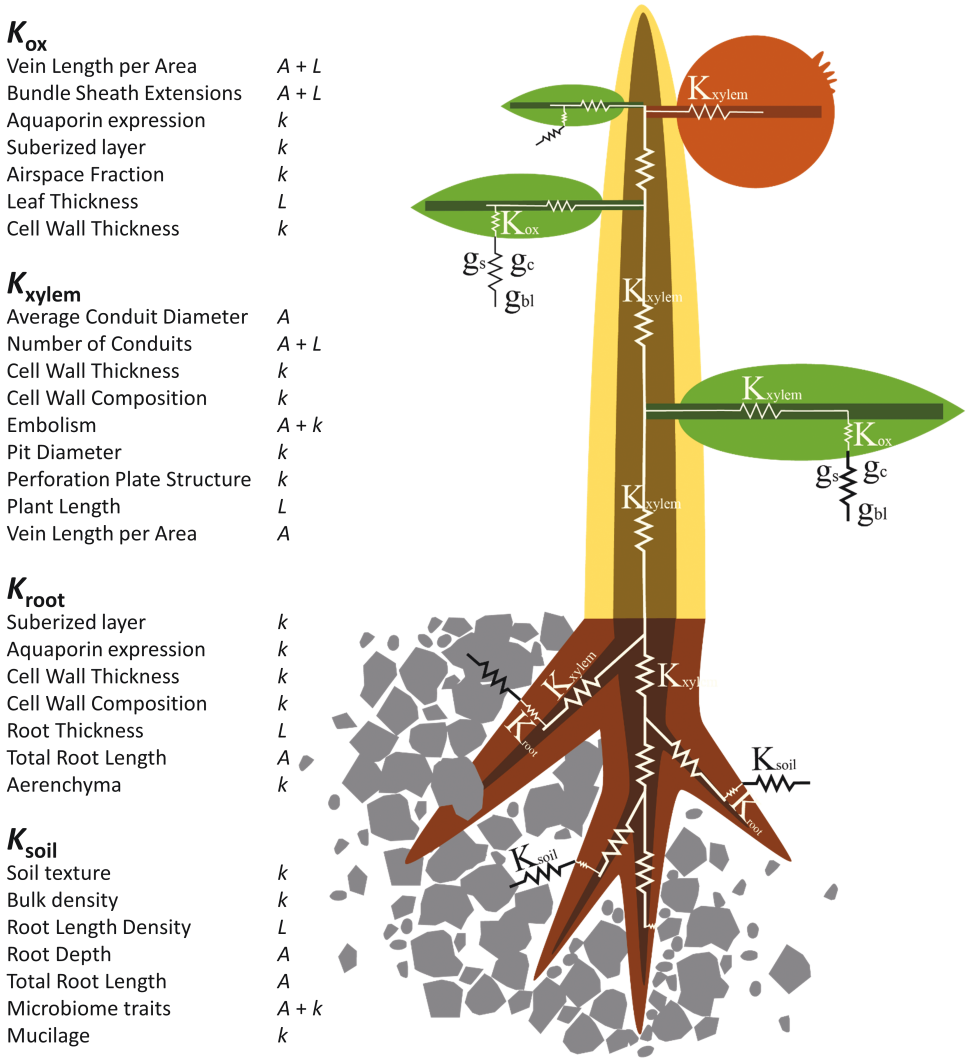

Figure 10. Anatomical and physiological traits affecting hydraulic conductance in different compartments along the transpiration stream. K_{soil}, K_{root}, K_{xylem}, K_{ox}, refer to soil, root, xylem and outside-xylem hydraulic conductances, respectively. For each of the four conductances, potentially influencing traits are listed, along with the corresponding parameter in equation (3.6), where A, k and L are the cross-sectional area, permeability and path length, respectively. g_s, g_c and g_{bl} are included in the graph for completeness and refer to the stomatal, the cuticular and the boundary-layer conductance to water vapour, respectively.

of conductance curves perfectly fit in the 'meta-mechanism' concept. As pointed out above, many different morphological and physiological traits at the cell and tissue level may impact this vulnerability, but the overall response function is valid across multiple environmental conditions (Venturas *et al.* 2017). To properly scale complexity, several examples exist where allometric links have been established. For example, Martre and Durand (2001) scaled the root hydraulic conductance to the total leaf area of the plant in a hydraulic model of tall fescue, and multiple FSPMs scale internode hydraulic conductance proportional to the internode's cross-sectional area and inversely proportional to the internode's length (da Silva *et al.* 2011; Nikinmaa *et al.* 2014; Coussement *et al.* 2020). This way, the number of parameters can be drastically reduced, while designing interesting and robust relations.

Despite the possibilities to keep models parsimonious, adding hydraulics comes with an increased need for data. Reliable plant hydraulics models need absolute and accurate water potential measurements for proper calibration and validation (Steppe 2018), but also to improve insights on the mechanisms to be modelled. Non-invasive and continuous measurements are preferred over destructive manual measurements, as these will enable better capturing the dynamics, which are required to fully understand mechanistic links between water potential and other physiological processes. In soil or growing media, the water potential can be continuously monitored using tensiometers (Jackisch *et al.* 2020). Recent advances in these technologies have enhanced the robustness of the signal and the operating range. In the plant, (leaf or stem) water potential can be destructively measured using the pressure chamber or

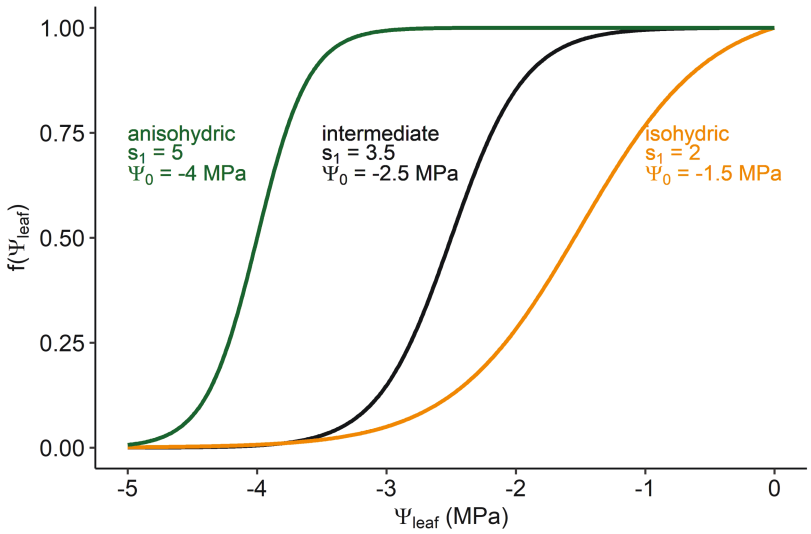

Figure 11. Example of sensitivity of stomatal conductance ($f(\Psi_{leaf})$) to leaf water potential Ψ_{leaf} implementation as a meta-mechanism in a plant or crop model. Results for equation (5.3) from Tuzet *et al.* (2003) with three different parameter combinations, showing anisohydric, intermediate and isohydric behaviour. Parameters s_1 [MPa^{-1}] and Ψ_0 [MPa] describe the sensitivity to the leaf water potential Ψ_{leaf} [MPa].

thermocouple psychrometry. The latter is also suitable for measuring osmotic potential (after freezing the sample) and is applied on smaller tissue parts, yet remains destructive and cumbersome. For woody stems, M. A. Dixon and Tyree (1984) developed a psychrometer for automatic and continuous monitoring of xylem water potential. Recently, Jain *et al.* (2021) developed a highly innovative, minimally invasive system to monitor leaf water potential. As this system allows to monitor the spatial distribution of water potential within the leaf, it may be suitable for calibrating and validating detailed extra-xylary leaf water transport and process-based stomatal conductance models (Buckley 2015; Buckley *et al.* 2015). Apart from direct measurements of water potential, continuously monitoring closely related variables like sap flow or turgor pressure strongly support hydraulic model development and verification. Currently, a wide variety of sap flow sensors is available for a wide range of stem sizes (Flo *et al.* 2019) and leaf turgor pressure can be recorded by leaf patch clamps (Zimmermann *et al.* 2008). Furthermore, monitoring organ dimensional changes at a high temporal resolution may prove very informative. In this respect, close links have been demonstrated between water potential dynamics and variations in stem diameter (De Swaef *et al.* 2015; Dietrich *et al.* 2018), leaf thickness (McBurney 1992) and LER (Tardieu *et al.* 2015; Barillot *et al.* 2021). Finally, novel 3D imaging techniques have become available to visualize water transport at multiple scales, including (synchrotron) X-ray tomography (Piovesan *et al.* 2021), neutron tomography and positron emission tomography (Hubeau and Steppe 2015). Such information is very useful for developing more accurate water transport models that take into account the actual 3D multiscale structure of the plant.

7. CONCLUSIONS

The primary use of water potential in plant models is to simulate water transport in the SPAC. As water potential is regarded the best indicator of plant water status, because it is the integrated result of above- and below-ground environmental conditions, it holds promise as a pivotal model variable to which other plant processes respond. We highlighted three ecophysiological processes, all of which have a well-recognized mechanistic link to water potential, that have been successfully implemented in plant hydraulic models: phloem transport, stomatal conductance and plant organ growth. These processes drive carbon allocation between source and sink (phloem transport), carbon assimilation (stomatal conductance) and water accumulation in growing tissues, and consequently build the bridge between plant water status and plant growth. Therefore, models that make this connection enable identification of crucial phenotypic traits for understanding (and potentially remediating) ecosystem resilience to drought and for breeding towards improved drought tolerance in crops. Therefore, we suggest that models at different scales (FSPM, CSM and TBM) would benefit from embedding hydraulics in their framework, especially when studying plant responses to drought.

ACKNOWLEDGEMENTS

The authors thank two anonymous reviewers for their constructive feedback. This work was initiated at the PlantComp 2020 workshop held in Gent.

CONTRIBUTIONS BY THE AUTHORS

T.D.S. did conceptualisation, investigation, writing - original draft preparation, writing - review & editing, visualization, project administration. O.P. contributed conceptualisation, writing - review & editing, project administration. S.A., I.B.S., W.C., P.L., B.N., and M.V.H. helped in investigation, writing - review & editing. V.C., L.P., and J.S. did investigation, writing - original draft preparation. S.G. contributed conceptualisation, writing - review & editing, visualization. C.S.C. did investigation, writing - original draft preparation, writing - review & editing. M.S. and F.w. helped in supervision, writing - review & editing, project administration.

SOURCES OF FUNDING

O.P. received PhD funding by Special Research Fund (BOF) of Ghent University (grant no. BOF17/DOC/324); S.A. received PhD funding by Research Foundation – Flanders (FWO) – FWO-Odysseus SiTeMan Project (grant no. G0F9216N); W.C. received PhD funding by Flanders Innovation and Entrepreneurship (grant no. VLAIO-LA 2017.0817) and the Horizon 2020 ERC Starting Grant (grant no. FORMICA 757833); V.C. was funded by the Fonds de la Recherche Scientifique – FNRS as a Postdoctoral researcher (grant no. 1208619F) and currently as FNRS Research associate; C.S.C. was funded by the Horizon 2020 EMPHASIS-Prep project (grant no. 739514). J.S. received PhD funding by Research Foundation – Flanders (FWO) (grant no. 1SE1921N); M.V.H. received PhD funding by Research Foundation – Flanders (FWO) – FWO-SBO Bisceps project (grant no. S007019N).

CONFLICT OF INTEREST

None declared.

LITERATURE CITED

Abera MK, Verboven P, Defraeye T, Fanta SW, Hertog ML, Carmeliet J, Nicolai BM. 2014a. A plant cell division algorithm based on cell biomechanics and ellipse-fitting. *Annals of Botany* **114**:605–617.

Abera MK, Verboven P, Herremans E, Defraeye T, Fanta SW, Ho QT, Carmeliet J, Nicolai BM. 2014b. 3D virtual pome fruit tissue generation based on cell growth modeling. *Food and Bioprocess Technology* **7**:542–555.

Agee E, He L, Bisht G, Couvreur V, Shahbaz P, Meunier F, Gough CM, Matheny AM, Bohrer G, Ivanov V. 2021. Root lateral interactions drive water uptake patterns under water limitation. *Advances in Water Resources* **151**:103896.

Albasha R, Fournier C, Pradal C, Chelle M, Prieto JA, Louarn G, Simonneau T, Lebon E. 2019. HydroShoot: a functional-structural plant model for simulating hydraulic structure, gas and energy exchange dynamics of complex plant canopies under water deficit—application to grapevine (*Vitis vinifera*). *In Silico Plants* **1**:diz007; doi:10.1093/insilicoplants/diz007

Anderegg WR. 2015. Spatial and temporal variation in plant hydraulic traits and their relevance for climate change impacts on vegetation. *The New Phytologist* **205**:1008–1014.

Anderegg WR, Berry JA, Field CB. 2012. Linking definitions, mechanisms, and modeling of drought-induced tree death. *Trends in Plant Science* **17**:693–700.

Anderegg WRL, Venturas MD. 2020. Plant hydraulics play a critical role in Earth system fluxes. *The New Phytologist* **226**:1535–1538.

Anderegg WRL, Wolf A, Arango-Velez A, Choat B, Chmura DJ, Jansen S, Kolb T, Li S, Meinzer F, Pita P, Resco de Dios V, Sperry JS, Wolfe BT, Pacala S. 2017. Plant water potential improves prediction of empirical stomatal models. *PLoS One* **12**:e0185481.

Aregawi WA, Abera MK, Fanta SW, Verboven P, Nicolai B. 2014. Prediction of water loss and viscoelastic deformation of apple tissue using a multi-scale model. *Journal of Physics: Condensed Matter* **26**:464111.

Arkebauer TJ, Norman JM, Sullivan CY. 1995. From cell growth to leaf growth: III. Kinetics of leaf expansion. *Agronomy Journal* **87**, 112–121.

Augé, R. M. 2001. Water relations, drought and vesicular-arbuscular mycorrhizal symbiosis. *Mycorrhiza* **11**:3–42.

Ball JT, Woodrow IE, Berry JA. 1987. A model predicting stomatal conductance and its contribution to the control of photosynthesis under different environmental conditions. In: Biggins J, ed. Progress in Photosynthesis Research: Volume 4 Proceedings of the VIIth International Congress on Photosynthesis, Providence, Rhode Island, USA, 10–15 August 1986. Dordrecht, The Netherlands: Springer, 221–224.

Barillot R, De Swaef T, Combes D, Durand JL, Escobar-Gutiérrez AJ, Martre P, Perrot C, Roy E, Frak E. 2021. Leaf elongation response to blue light is mediated by stomatal-induced variations in transpiration in *Festuca arundinacea*. *Journal of Experimental Botany* **72**:2642–2656.

Beerling DJ, Franks PJ. 2010. Plant science: the hidden cost of transpiration. *Nature* **464**:495–496.

Bisht G, Riley WJ. 2019. Development and verification of a numerical library for solving global terrestrial multiphysics problems. *Journal of Advances in Modeling Earth Systems* **11**:1516–1542.

Bouda M, Brodersen C, Saiers J. 2018. Whole root system water conductance responds to both axial and radial traits and network topology over natural range of trait variation. *Journal of Theoretical Biology* **456**:49–61.

Bret-Harte MS, Silk WK. 1994. Nonvascular, symplasmic diffusion of sucrose cannot satisfy the carbon demands of growth in the primary root tip of *Zea mays* L. *Plant Physiology* **105**:19–33.

Briggs GE. 1967. *Movement of water in plants*. Oxford: Blackwell Scientific.

Brodribb TJ, McAdam SAM. 2017. Evolution of the stomatal regulation of plant water content. *Plant Physiology* **174**:639–649.

Buckingham E, United States Department of Agriculture, Bureau of Soils. 1907. *Studies on the movement of soil moisture*. Washington, DC: Govt. Print. Off.

Buckley TN. 2005. The control of stomata by water balance. *The New Phytologist* **168**:275–292.

Buckley TN. 2015. The contributions of apoplastic, symplastic and gas phase pathways for water transport outside the bundle sheath in leaves. *Plant, Cell & Environment* **38**:7–22.

Buckley TN. 2017. Modeling stomatal conductance. *Plant Physiology* **174**:572–582.

Buckley TN, John GP, Scoffoni C, Sack L. 2015. How does leaf anatomy influence water transport outside the xylem? *Plant Physiology* **168**:1616–1635.

Buckley TN, Mott KA, Farquhar GD. 2003. A hydromechanical and biochemical model of stomatal conductance. *Plant, Cell & Environment* **26**:1767–1785.

Buckley TN, Turnbull TL, Adams MA. 2012. Simple models for stomatal conductance derived from a process model: cross-validation against sap flux data. *Plant, Cell & Environment* **35**:1647–1662.

Cabon A, Peters RL, Fonti P, Martínez-Vilalta J, De Cáceres M. 2020. Temperature and water potential co-limit stem cambial activity along a steep elevational gradient. *The New Phytologist* **226**:1325–1340.

Cabrita P, Thorpe M, Huber G. 2013. Hydrodynamics of steady state phloem transport with radial leakage of solute. *Frontiers in Plant Science* **4**:531.

Caldeira CF, Bosio M, Parent B, Jeanguenin L, Chaumont F, Tardieu F. 2014. A hydraulic model is compatible with rapid changes in leaf elongation under fluctuating evaporative demand and soil water status. *Plant Physiology* **164**:1718–1730.

Cardoso AA, Brodribb TJ, Lucani CJ, DaMatta FM, McAdam SAM. 2018. Coordinated plasticity maintains hydraulic safety in sunflower leaves. *Plant, Cell & Environment* **41**:2567–2576.

Carminati A. 2012. A model of root water uptake coupled with rhizosphere dynamics. *Vadose Zone Journal* **11**:vzj2011.0106.

Carminati A, Javaux M. 2020. Soil rather than xylem vulnerability controls stomatal response to drought. *Trends in Plant Science* **25**:868–880.

Carpita NC, Gibeaut DM. 1993. Structural models of primary cell walls in flowering plants: consistency of molecular structure with the physical properties of the walls during growth. *The Plant Journal* **3**:1–30.

Charrier G. 2020. Extrapolating physiological response to drought through step-by-step analysis of water potential. *Plant Physiology* **184**:560–561.

Chaumont F, Tyerman SD. 2014. Aquaporins: highly regulated channels controlling plant water relations. *Plant Physiology* **164**:1600–1618.

Chelle M, Andrieu B. 1998. The nested radiosity model for the distribution of light within plant canopies. *Ecological Modelling* **111**:75–91.

Chen J, Beauvoit B, Génard M, Colombié S, Moing A, Vercambre G, Gomès E, Gibon Y, Dai Z. 2021. Modelling predicts tomatoes can be bigger and sweeter if biophysical factors and transmembrane transports are fine-tuned during fruit development. *The New Phytologist* **230**:1489–1502.

Choat B, Brodribb TJ, Brodersen CR, Duursma RA, López R, Medlyn BE. 2018. Triggers of tree mortality under drought. *Nature* **558**:531–539.

Choat B, Jansen S, Brodribb TJ, Cochard H, Delzon S, Bhaskar R, Bucci SJ, Feild TS, Gleason SM, Hacke UG, Jacobsen AL, Lens F, Maherali H, Martínez-Vilalta J, Mayr S, Mencuccini M, Mitchell PJ, Nardini A, Pittermann J, Pratt RB, Sperry JS, Westoby M, Wright IJ, Zanne AE. 2012. Global convergence in the vulnerability of forests to drought. *Nature* **491**:752–755.

Christoffersen BO, Gloor M, Fauset S, Fyllas NM, Galbraith DR, Baker TR, Kruijt B, Rowland L, Fisher RA, Binks OJ, Sevanto S, Xu C, Jansen S, Choat B, Mencuccini M, McDowell NG, Meir P. 2016. Linking hydraulic traits to tropical forest function in a size-structured and trait-driven model (TFS v.1-Hydro). *Geoscientific Model Development* **9**:4227–4255.

Christy AL, Ferrier JM. 1973. A mathematical treatment of Munch's pressure-flow hypothesis of phloem translocation. *Plant Physiology* **52**:531–538.

Cochard H, Badel E, Herbette S, Delzon S, Choat B, Jansen S. 2013. Methods for measuring plant vulnerability to cavitation: a critical review. *Journal of Experimental Botany* **64**:4779–4791.

Cochard H, Pimont F, Ruffault J, Martin-StPaul N. 2021. SurEau: a mechanistic model of plant water relations under extreme drought. *Annals of Forest Science* **78**:55.

Cochard H, Venisse JS, Barigah TS, Brunel N, Herbette S, Guilliot A, Tyree MT, Sakr S. 2007. Putative role of aquaporins in variable hydraulic conductance of leaves in response to light. *Plant Physiology* **143**:122–133.

Collins B, Chapman S, Hammer G, Chenu K. 2021. Limiting transpiration rate in high evaporative demand conditions to improve Australian wheat productivity. *In Silico Plants* **3**:diab006; doi:10.1093/insilicoplants/diab006

Cooke JR, De Baerdemaeker JG, Rand RH, Mang HA. 1976. A finite element shell analysis of guard cell deformations. *Transactions of the ASAE* **19**:1107–1121.

Cooper M, Powell O, Voss-Fels KP, Messina CD, Gho C, Podlich DW, Technow F, Chapman SC, Beveridge CA, Ortiz-Barrientos D, Hammer GL. 2021. Modelling selection response in plant-breeding programs using crop models as mechanistic gene-to-phenotype (CGM-G2P) multi-trait link functions. *In Silico Plants* **3**:diaa016; doi:10.1093/insilicoplants/diaa016

Cosgrove DJ. 1993. Wall extensibility: its nature, measurement and relationship to plant cell growth. *The New Phytologist* **124**:1–23.

Cosgrove DJ. 2005. Growth of the plant cell wall. *Nature Reviews Molecular Cell Biology* **6**:850–861.

Coussement JR, De Swaef T, Lootens P, Roldán-Ruiz I, Steppe K. 2018. Introducing turgor-driven growth dynamics into functional-structural plant models. *Annals of Botany* **121**:849–861.

Coussement JR, De Swaef T, Lootens P, Steppe K. 2020. Turgor-driven plant growth applied in a soybean functional-structural plant model. *Annals of Botany* **126**:729–744.

Coussement JR, Villers SLY, Nelissen H, Inzé D, Steppe K. 2021. Turgor-time controls grass leaf elongation rate and duration under drought stress. *Plant, Cell & Environment* **44**:1361–1378.

Couvreur V, Faget M, Lobet G, Javaux M, Chaumont F, Draye X. 2018. Going with the flow: multiscale insights into the composite nature of water transport in roots. *Plant Physiology* **178**:1689–1703.

Couvreur V, Heymans A, Lobet G, Draye X. 2021. Evidence for a multicellular symplasmic water pumping mechanism across vascular plant roots. *bioRxiv*, doi:10.1101/2021.04.19.439789.

Couvreur V, Vanderborght J, Beff L, Javaux M. 2014. Horizontal soil water potential heterogeneity: simplifying approaches for crop water dynamics models. *Hydrology and Earth System Sciences* **18**:1723–1743.

Cowan IR. 1965. Transport of water in the soil-plant-atmosphere system. *Journal of Applied Ecology* **2**:221–239.

Cowan IR, Farquhar GD. 1977. Stomatal function in relation to leaf metabolism and environment. *Symposia of the Society for Experimental Biology* **31**:471–505.

Cuneo IF, Barrios-Masias F, Knipfer T, Uretsky J, Reyes C, Lenain P, Brodersen CR, Walker MA, McElrone AJ. 2021. Differences in grapevine rootstock sensitivity and recovery from drought are linked to fine root cortical lacunae and root tip function. *The New Phytologist* **229**:272–283.

Damour G, Simonneau T, Cochard H, Urban L. 2010. An overview of models of stomatal conductance at the leaf level. *Plant, Cell & Environment* **33**:1419–1438.

Darcy H. 1856. *Les fontaines publiques de la ville de Dijon: exposition et application des principes a suivre et des formules a employer dans les questions de distribution d'eau; ouvrage terminé par un appendice relatif aux fournitures d'eau de plusieurs villes au filtrage des eaux et a la fabrication des tuyaux de fonte, de plomb, de tole et de bitume*. Paris: Victor Dalmont, Libraire des Corps imperiaux des ponts et chaussées et des mines.

Da Silva D, Favreau R, Auzmendi I, DeJong TM. 2011. Linking water stress effects on carbon partitioning by introducing a xylem circuit into L-PEACH. *Annals of Botany* **108**:1135–1145.

Daudet FA, Lacointe A, Gaudillère JP, Cruiziat P. 2002. Generalized Münch coupling between sugar and water fluxes for modelling carbon allocation as affected by water status. *Journal of Theoretical Biology* **214**:481–498.

Dauzat J, Rapidel B, Berger A. 2001. Simulation of leaf transpiration and sap flow in virtual plants: model description and application to

a coffee plantation in Costa Rica. *Agricultural and Forest Meteorology* **109**:143–160.

De Schepper V, De Swaef T, Bauweraerts I, Steppe K. 2013. Phloem transport: a review of mechanisms and controls. *Journal of Experimental Botany* **64**:4839–4850.

De Schepper V, Steppe K. 2010. Development and verification of a water and sugar transport model using measured stem diameter variations. *Journal of Experimental Botany* **61**:2083–2099.

De Schepper V, Steppe K, Van Labeke M-C, Lemeur R. 2010. Detailed analysis of double girdling effects on stem diameter variations and sap ow in young oak trees. *Environmental and Experimental Botany* **68**:149–156.

De Swaef T, De Schepper V, Vandegehuchte MW, Steppe K. 2015. Stem diameter variations as a versatile research tool in ecophysiology. *Tree Physiology* **35**:1047–1061.

De Swaef T, Driever SM, Van Meulebroek L, Vanhaecke L, Marcelis LF, Steppe K. 2013. Understanding the effect of carbon status on stem diameter variations. *Annals of Botany* **111**:31–46.

De Swaef T, Steppe K. 2010. Linking stem diameter variations to sap flow, turgor and water potential in tomato. *Functional Plant Biology* **37**:429–438.

Deans RM, Brodribb TJ, Busch FA, Farquhar GD. 2020. Optimization can provide the fundamental link between leaf photosynthesis, gas exchange and water relations. *Nature Plants* **6**:1116–1125.

de Groot BL, Grubmüller H. 2001. Water permeation across biological membranes: mechanism and dynamics of aquaporin-1 and GlpF. *Science* **294**:2353–2357.

Devi MJ, Reddy VR. 2020. Stomatal closure response to soil drying at different vapor pressure deficit conditions in maize. *Plant Physiology and Biochemistry* **154**:714–722.

Dewar RC. 1993. A root-shoot partitioning model based on carbon-nitrogen-water interactions and Munch phloem flow. *Functional Ecology* **7**:356–368.

Dewar RC. 2002. The Ball–Berry–Leuning and Tardieu–Davies stomatal models: synthesis and extension within a spatially aggregated picture of guard cell function. *Plant, Cell & Environment*, **25**, 1383–1398.

Diaz-Espejo A, Buckley TN, Sperry JS, Cuevas MV, de Cires A, Elsayed-Farag S, Martin-Palomo MJ, Muriel JL, Perez-Martin A, Rodriguez-Dominguez CM, Rubio-Casal AE, Torres-Ruiz JM, Fernández JE. 2012. Steps toward an improvement in process-based models of water use by fruit trees: a case study in olive. *Agricultural Water Management* **114**:37–49.

Diels E, Wang Z, Nicolai B, Ramon H, Smeets B. 2019. Discrete element modelling of tomato tissue deformation and failure at the cellular scale. *Soft Matter* **15**:3362–3378.

Dietrich L, Zweifel R, Kahmen A. 2018. Daily stem diameter variations can predict the canopy water status of mature temperate trees. *Tree Physiology* **38**:941–952.

Ding L, Milhiet T, Couvreur V, Nelissen H, Meziane A, Parent B, Aesaert S, Van Lijsebettens M, Inzé D, Tardieu F, Draye X, Chaumont F. 2020. Modification of the expression of the aquaporin ZmPIP2;5 affects water relations and plant growth. *Plant Physiology* **182**:2154–2165.

Dixon HH, Joly J. 1895. On the ascent of sap. *Philosophical Transactions of the Royal Society of London. B: Biological Sciences* **186**:563–576.

Dixon MA, Tyree MT. 1984. A new stem hygrometer, corrected for temperature gradients and calibrated against the pressure bomb. *Plant, Cell & Environment* **7**:693–697.

Doussan C, Pierret A, Garrigues E, Pagès L. 2006. Water uptake by plant roots: II—modelling of water transfer in the soil root-system with explicit account of flow within the root system—comparison with experiments. *Plant and Soil* **283**:99–117.

Duursma RA, Blackman CJ, Lopéz R, Martin-StPaul NK, Cochard H, Medlyn BE. 2019. On the minimum leaf conductance: its role in models of plant water use, and ecological and environmental controls. *The New Phytologist* **221**:693–705.

Earles JM, Buckley TN, Brodersen CR, Busch FA, Cano FJ, Choat B, Evans JR, Farquhar GD, Harwood R, Huynh M, John GP, Miller ML, Rockwell FE, Sack L, Scoffoni C, Struik PC, Wu A, Yin X, Barbour MM. 2019. Embracing 3D complexity in leaf carbon-water exchange. *Trends in Plant Science* **24**:15–24.

Eller CB, Rowland L, Mencuccini M, Rosas T, Williams K, Harper A, Medlyn BE, Wagner Y, Klein T, Teodoro GS, Oliveira RS, Matos IS, Rosado BHP, Fuchs K, Wohlfahrt G, Montagnani L, Meir P, Sitch S, Cox PM. 2020. Stomatal optimization based on xylem hydraulics (SOX) improves land surface model simulation of vegetation responses to climate. *The New Phytologist* **226**:1622–1637.

Fanta SW, Abera MK, Aregawi WA, Ho QT, Verboven P, Carmeliet J, Nicolai BM. 2014. Microscale modeling of coupled water transport and mechanical deformation of fruit tissue during dehydration. *Journal of Food Engineering* **124**:86–96.

Fatichi S, Pappas C, Ivanov VY. 2016. Modeling plant–water interactions: an ecohydrological overview from the cell to the global scale. *WIREs Water* **3**:327–368.

Ferrier JM, Tyree MT, Christy AL. 1975. The theoretical time-dependent behavior of a Münch pressure-flow system: the effect of sinusoidal time variation in sucrose loading and water potential. *Canadian Journal of Botany* **53**:1120–1127.

Fishman S, Génard M. 1998. A biophysical model of fruit growth: simulation of seasonal and diurnal dynamics of mass. *Plant, Cell & Environment* **21**:739–752.

Flo V, Martinez-Vilalta J, Steppe K, Schuldt B, Poyatos R. 2019. A synthesis of bias and uncertainty in sap flow methods. *Agricultural and Forest Meteorology* **271**:362–374.

Foster KJ, Miklavcic SJ. 2017. A comprehensive biophysical model of ion and water transport in plant roots. I. Clarifying the roles of endodermal barriers in the salt stress response. *Frontiers in Plant Science* **8**:1326.

Foster KJ, Miklavcic SJ. 2020. A comprehensive biophysical model of ion and water transport in plant roots. III. Quantifying the energy costs of ion transport in salt-stressed roots of *Arabidopsis*. *Frontiers in Plant Science* **11**:865.

Franks PJ. 2004. Stomatal control and hydraulic conductance, with special reference to tall trees. *Tree Physiology* **24**:865–878.

Gambetta GA, Fei J, Rost TL, Knipfer T, Matthews MA, Shackel KA, Walker MA, McElrone AJ. 2013. Water uptake along the length of grapevine fine roots: developmental anatomy, tissue-specific aquaporin expression, and pathways of water transport. *Plant Physiology* **163**:1254–1265.

Gambetta GA, Knipfer T, Fricke W, McElrone AJ. 2017. Aquaporins and root water uptake. In: Chaumont F, Tyerman SD, eds. *Plant aquaporins: from transport to signaling*. Cham: Springer International Publishing, 133–153.

Gardner WR. 1960. Dynamic aspects of water availability to plants. *Soil Science* **89**:63–73.

Génard M, Bertin N, Borel C, Bussières P, Gautier H, Habib R, Léchaudel M, Lecomte A, Lescourret F, Lobit P, Quilot B. 2007. Towards a virtual fruit focusing on quality: modelling features and potential uses. *Journal of Experimental Botany* **58**:917–928.

Génard M, Fishman S, Vercambre G, Huguet JG, Bussi C, Besset J, Habib R. 2001. A biophysical analysis of stem and root diameter variations in woody plants. *Plant Physiology* **126**:188–202.

Gradmann H. 1928. Untersuchungen Über die Wasserverhältnisse des Bodens als Grundlage des Pflanzenwachstums. *Jahrbücher für Wissenschaftliche Botanik* **69**:1.

Hacke UG, Sperry JS. 2001. Functional and ecological xylem anatomy. *Perspectives in Plant Ecology Evolution and Systematics* **4**:97–115.

Hall AJ, Minchin PE. 2013. A closed-form solution for steady-state coupled phloem/xylem flow using the Lambert-W function. *Plant, Cell & Environment* **36**:2150–2162.

Hammer G, Cooper M, Tardieu F, Welch S, Walsh B, van Eeuwijk F, Chapman S, Podlich D. 2006. Models for navigating biological complexity in breeding improved crop plants. *Trends in Plant Science* **11**:587–593.

Hammond GE, Lichtner PC, Mills RT. 2014. Evaluating the performance of parallel subsurface simulators: an illustrative example with PFLOTRAN. *Water Resources Research* **50**:208–228.

Hari P, Mäkelä A, Korpilahti E, Holmberg M. 1986. Optimal control of gas exchange. *Tree Physiology* **2**:169–175.

He D, Wang E, Wang J, Robertson MJ. 2017. Data requirement for effective calibration of process-based crop models. *Agricultural and Forest Meteorology* **234–235**:136–148.

Henke M, Buck-Sorlin GH. 2017. Using a full spectral raytracer for calculating light microclimate in functional-structural plant modelling. *Computing and Informatics* **36**:1492–1522.

Henry A, Cal AJ, Batoto TC, Torres RO, Serraj R. 2012. Root attributes affecting water uptake of rice (*Oryza sativa*) under drought. *Journal of Experimental Botany* **63**:4751–4763.

Heymans A, Couvreur V, LaRue T, Paez-Garcia A, Lobet G. 2020. GRANAR, a computational tool to better understand the functional importance of monocotyledon root anatomy. *Plant Physiology* **182**:707–720.

Hills A, Chen ZH, Amtmann A, Blatt MR, Lew VL. 2012. OnGuard, a computational platform for quantitative kinetic modeling of guard cell physiology. *Plant Physiology* **159**:1026–1042.

Hilty J, Muller B, Pantin F, Leuzinger S. 2021. Plant growth: the what, the how, and the why. *The New Phytologist* **232**:25–41.

Hishi T. 2007. Heterogeneity of individual roots within the fine root architecture: causal links between physiological and ecosystem functions. *Journal of Forest Research* **12**:126–133.

Hochberg U, Rockwell FE, Holbrook NM, Cochard H. 2018. Iso/anisohydry: a plant–environment interaction rather than a simple hydraulic trait. *Trends in Plant Science* **23**:112–120.

Holbrook NM, Zwieniecki MA. 1999. Embolism repair and xylem tension: do we need a miracle? *Plant Physiology* **120**:7–10.

Holloway-Phillips MM, Brodribb TJ. 2011. Minimum hydraulic safety leads to maximum water-use efficiency in a forage grass. *Plant, Cell & Environment* **34**:302–313.

Hölttä T, Mencuccini M, Nikinmaa E. 2009. Linking phloem function to structure: analysis with a coupled xylem-phloem transport model. *Journal of Theoretical Biology* **259**:325–337.

Hölttä T, Vesala T, Sevanto S, Perämäki M, Nikinmaa E. 2006. Modeling xylem and phloem water ows in trees according to cohesion theory and Münch hypothesis. *Trees* **20**:67–78.

Hoogenboom G, Justes E, Pradal C, Launay M, Asseng S, Ewert F, Martre P. 2021. Icropm 2020: crop modeling for the future. *The Journal of Agricultural Science* **158**:791–793.

Hubeau M, Steppe K. 2015. Plant-PET scans: in vivo mapping of xylem and phloem functioning. *Trends in Plant Science* **20**:676–685.

Hunt ER, Running SW, Federer CA. 1991. Extrapolating plant water flow resistances and capacitances to regional scales. *Agricultural and Forest Meteorology* **54**:169–195.

Jackisch C, Germer K, Graeff T, Andrä, I., Schulz K, Schiedung M, Haller-Jans J, Schneider J, Jaquemotte J, Helmer P, Lotz L, Bauer A, Hahn I, Šanda M, Kumpan M, Dorner J, de Rooij G, Wessel-Bothe S, Kottmann L, Schittenhelm S, Durner W. 2020. Soil moisture and matric potential—an open field comparison of sensor systems. *Earth System Science Data* **12**:683–697.

Jacobsen AL, Pratt RB, Ewers FW, Davis SD. 2007. Cavitation resistance among 26 chaparral species of southern California. *Ecological Monographs* **77**:99–115.

Jain P, Liu W, Zhu S, Chang CY-Y., Melkonian J, Rockwell FE, Pauli D, Sun Y, Zipfel WR, Holbrook NM, Riha SJ, Gore MA, Stroock AD. 2021. A minimally disruptive method for measuring water potential in planta using hydrogel nanoreporters. *Proceedings of the National Academy of Sciences of the United States of America* **118**:23.

Jarvis PG, Monteith JL, Weatherley PE. 1976. The interpretation of the variations in leaf water potential and stomatal conductance found in canopies in the field. *Philosophical Transactions of the Royal Society of London. B, Biological Sciences* **273**:593–610.

Jasechko S, Sharp ZD, Gibson JJ, Birks SJ, Yi Y, Fawcett PJ. 2013. Terrestrial water fluxes dominated by transpiration. *Nature* **496**:347–350.

Javaux M, Carminati A. 2021. Soil hydraulics affect the degree of isohydricity. *Plant Physiology* **186**:1378–1381.

Javaux M, Couvreur V, Vanderborght J, Vereecken H. 2013. Root water uptake: from three-dimensional biophysical processes to macroscopic modeling approaches. *Vadose Zone Journal* **12**:4.

Javaux M, Schröder T, Vanderborght J, Vereecken H. 2008. Use of a three-dimensional detailed modeling approach for predicting root water uptake. *Vadose Zone Journal* **7**:1079–1088.

Jensen KH. 2018. Phloem physics: mechanisms, constraints, and perspectives. *Current Opinion in Plant Biology* **43**:96–100.

Jensen KH, Mullendore DL, Holbrook NM, Bohr T, Knoblauch M, Bruus H. 2012. Modeling the hydrodynamics of phloem sieve plates. *Frontiers in Plant Science* **3**:151.

Jin Z, Zhuang Q, Tan Z, Dukes JS, Zheng B, Melillo JM. 2016. Do maize models capture the impacts of heat and drought stresses on yield? Using algorithm ensembles to identify successful approaches. *Global Change Biology* **22**:3112–3126.

Jones HG. 2015. *Plants and microclimate: a quantitative approach to environmental plant physiology*. Cambridge: Cambridge University Press.

Jones J, Hoogenboom G, Porter C, Boote K, Batchelor W, Hunt L, Wilkens P, Singh U, Gijsman A, Ritchie J. 2003. The DSSAT cropping system model. *European Journal of Agronomy* **18**:235–265.

Kennedy D, Swenson S, Oleson KW, Lawrence DM, Fisher R, da Costa ACL, Gentine P. 2019. Implementing plant hydraulics

in the community land model, version 5. *Journal of Advances in Modeling Earth Systems* **11**:485–513.

Knipfer T, Besse M, Verdeil JL, Fricke W. 2011. Aquaporin-facilitated water uptake in barley (*Hordeum vulgare* L.) roots. *Journal of Experimental Botany* **62**:4115–4126.

Kramer PJ, Boyer JS. 1995. *Water relations of plants and soils*. San Diego: Academic Press.

Kroener E, Zarebanadkouki M, Kaestner A, Carminati A. 2014. Nonequilibrium water dynamics in the rhizosphere: how mucilage affects water flow in soils. *Water Resources Research* **50**:6479–6495.

Lacointe A, Minchin PEH. 2008. Modelling phloem and xylem transport within a complex architecture. *Functional Plant Biology* **35**:772–780.

Lechaudel M, Vercambre G, Lescourret F, Normand F, Génard M. 2007. An analysis of elastic and plastic fruit growth of mango in response to various assimilate supplies. *Tree Physiology* **27**:219–230.

Lescourret F, Génard M. 2005. A virtual peach fruit model simulating changes in fruit quality during the final stage of fruit growth. *Tree Physiology* **25**:1303–1315.

Lesk C, Rowhani P, Ramankutty N. 2016. Influence of extreme weather disasters on global crop production. *Nature* **529**:84–87.

Leuning R. 1995. A critical appraisal of a combined stomatal-photosynthesis model for C_3 plants. *Plant, Cell & Environment* **18**:339–355.

Liu HF, Génard M, Guichard S, Bertin N. 2007. Model-assisted analysis of tomato fruit growth in relation to carbon and water fluxes. *Journal of Experimental Botany* **58**:3567–3580.

Liu Y, Wu L, Baddeley JA, Watson CA. 2011. Models of biological nitrogen fixation of legumes. A review. *Agronomy for Sustainable Development* **31**:155–172.

Lobet G, Couvreur V, Meunier F, Javaux M, Draye X. 2014. Plant water uptake in drying soils. *Plant Physiology* **164**:1619–1627.

Lockhart JA. 1965. An analysis of irreversible plant cell elongation. *Journal of Theoretical Biology* **8**:264–275.

López R, Cano FJ, Martin-StPaul NK, Cochard H, Choat B. 2021. Coordination of stem and leaf traits define different strategies to regulate water loss and tolerance ranges to aridity. *The New Phytologist* **230**:497–509.

Ma F, Peterson CA. 2001. Frequencies of plasmodesmata in *Allium cepa* L. roots: implications for solute transport pathways. *Journal of Experimental Botany* **52**:1051–1061.

Martinez-Vilalta J, Piñol J, Beven K. 2002. A hydraulic model to predict drought-induced mortality in woody plants: an application to climate change in the Mediterranean. *Ecological Modelling* **155**:127–147.

Martínez-Vilalta J, Poyatos R, Aguadé D, Retana J, Mencuccini M. 2014. A new look at water transport regulation in plants. *The New Phytologist* **204**:105–115.

Martin-StPaul N, Delzon S, Cochard H. 2017. Plant resistance to drought depends on timely stomatal closure. *Ecology Letters* **20**:1437–1447.

Martre P, Durand J-L. 2001. Quantitative analysis of vasculature in the leaves of *Festuca arundinacea* (Poaceae): implications for axial water transport. *International Journal of Plant Sciences* **162**:755–766.

Martre P, Durand JL, Cochard H. 2000. Changes in axial hydraulic conductivity along elongating leaf blades in relation to xylem maturation in tall fescue. *The New Phytologist* **146**:235–247.

Martre P, Quilot-Turion B, Luquet D, Memmah M-MO-S, Chenu K, Debaeke P. 2015. Model-assisted phenotyping and ideotype design. In: Sadras VO, Calderini DF, eds. *Crop physiology*. San Diego: Academic Press, 349–373.

McBurney T. 1992. The relationship between leaf thickness and plant water potential. *Journal of Experimental Botany* **43**:327–335.

Medlyn BE, Duursma RA, Eamus D, Ellsworth DS, Prentice IC, Barton CVM, Crous KY, Angelis PD, Freeman M, Wingate L. 2011. Reconciling the optimal and empirical approaches to modelling stomatal conductance. *Global Change Biology* **17**:2134–2144.

Mencuccini M, Manzoni S, Christoffersen B. 2019. Modelling water fluxes in plants: from tissues to biosphere. *The New Phytologist* **222**:1207–1222.

Michel BE. 1972. Solute potentials of sucrose solutions. *Plant Physiology* **50**:196–198.

Minchin PEH, Lacointe A. 2017. Consequences of phloem pathway unloading/reloading on equilibrium flows between source and sink: a modelling approach. *Functional Plant Biology* **44**:507–514.

Minchin PEH, Thorpe MR, Farrar JF. 1993. A simple mechanistic model of phloem transport which explains sink priority. *Journal of Experimental Botany* **44**:947–955.

Muller B, Pantin F, Génard M, Turc O, Freixes S, Piques M, Gibon Y. 2011. Water deficits uncouple growth from photosynthesis, increase C content, and modify the relationships between C and growth in sink organs. *Journal of Experimental Botany* **62**:1715–1729.

Münch E. 1930. *Die stoffbewegungen in der pflanze*. Jena: G. Fischer.

Myburg AA, Lev-Yadun S, Sederoff RR. 2013. Xylem structure and function. In: eLS. Hoboken, NJ: John Wiley & Sons, Ltd.

Nikinmaa E, Sievänen R, Hölttä T. 2014. Dynamics of leaf gas exchange, xylem and phloem transport, water potential and carbohydrate concentration in a realistic 3-D model tree crown. *Annals of Botany* **114**:653–666.

Nikolov NT, Massman WJ, Schoettle AW. 1995. Coupling biochemical and biophysical processes at the leaf level: an equilibrium photosynthesis model for leaves of C_3 plants. *Ecological Modelling* **80**:205–235.

Nobel PS. 1983. *Biophysical plant physiology and ecology*. San Francisco: W.H. Freeman and Company.

North GB, Martre P, Nobel PS. 2004. Aquaporins account for variations in hydraulic conductance for metabolically active root regions of *Agave deserti* in wet, dry, and rewetted soil. *Plant, Cell & Environment* **27**:219–228.

Or D, Lehmann P, Shahraeeni E, Shokri N. 2013. Advances in soil evaporation physics—a review. *Vadose Zone Journal* **12**:vzj2012.0163.

Ortega JK. 1985. Augmented growth equation for cell wall expansion. *Plant Physiology* **79**:318–320.

Pammenter NW, Vander Willigen C. 1998. A mathematical and statistical analysis of the curves illustrating vulnerability of xylem to cavitation. *Tree Physiology* **18**:589–593.

Parent B, Tardieu F. 2014. Can current crop models be used in the phenotyping era for predicting the genetic variability of yield of plants subjected to drought or high temperature? *Journal of Experimental Botany* **65**:6179–6189.

Passioura JB. 1980. The meaning of matric potential. *Journal of Experimental Botany* **31**:1161–1169.

Passot S, Gnacko F, Moukouanga D, Lucas M, Guyomarc'h S, Ortega BM, Atkinson JA, Belko MN, Bennett MJ, Gantet P, Wells DM, Guédon Y, Vigouroux Y, Verdeil J-L, Muller B, Laplaze L. 2016. Characterization of pearl millet root architecture

and anatomy reveals three types of lateral roots. *Frontiers in Plant Science* **7**.

Peng B, Guan K, Tang J, Ainsworth EA, Asseng S, Bernacchi CJ, Cooper M, Delucia EH, Elliott JW, Ewert F, Grant RF, Gustafson DI, Hammer GL, Jin Z, Jones JW, Kimm H, Lawrence DM, Li Y, Lombardozzi DL, Marshall-Colon A, Messina CD, Ort DR, Schnable JC, Vallejos CE, Wu A, Yin X, Zhou W. 2020. Towards a multiscale crop modelling framework for climate change adaptation assessment. *Nature Plants* **6**:338–348.

Perämäki M, Nikinmaa E, Sevanto S, Ilvesniemi H, Siivola E, Hari P, Vesala T. 2001. Tree stem diameter variations and transpiration in Scots pine: an analysis using a dynamic sap flow model. *Tree Physiology* **21**:889–897.

Peterson CA, Cholewa E. 1998. Structural modifications of the apoplast and their potential impact on ion uptake. *Zeitschrift für Pflanzenernährung und Bodenkunde* **161**:521–531.

Piovesan A, Vancauwenberghe V, Van De Looverbosch T, Verboven P, Nicolaï B. 2021. X-ray computed tomography for 3D plant imaging. *Trends in Plant Science* **26**:1171–1185.

Postma JA, Kuppe C, Owen MR, Mellor N, Griffiths M, Bennett MJ, Lynch JP, Watt M. 2017. OpenSimRoot: widening the scope and application of root architectural models. *The New Phytologist* **215**:1274–1286.

Pound MP, French AP, Wells DM, Bennett MJ, Pridmore TP. 2012. CellSeT: novel software to extract and analyze structured networks of plant cells from confocal images. *The Plant Cell* **24**:1353–1361.

Proseus TE, Boyer JS. 2006. Periplasm turgor pressure controls wall deposition and assembly in growing *Chara corallina* cells. *Annals of Botany* **98**:93–105.

Proseus TE, Ortega JK, Boyer JS. 1999. Separating growth from elastic deformation during cell enlargement. *Plant Physiology* **119**:775–784.

Pusch W, Woermann D. 1970. Study of the interrelation between reflection coefficient and solute rejection efficiency using a strong basic anion exchange membrane. *Berichte der Bunsengesellschaft für Physikalische Chemie* **74**:444–449.

Ray PM, Green PB, Cleland R. 1972. Role of turgor in plant cell growth. *Nature* **239**:163–164.

Rewald B, Ephrath JE, Rachmilevitch S. 2011. A root is a root is a root? Water uptake rates of Citrus root orders. *Plant, Cell & Environment* **34**:33–42.

Richards LA. 1931. Capillary conduction of liquids through porous mediums. *Physics* **1**:318–333.

Rodriguez-Dominguez CM, Buckley TN, Egea G, de Cires A, Hernandez-Santana V, Martorell S, Diaz-Espejo A. 2016. Most stomatal closure in woody species under moderate drought can be explained by stomatal responses to leaf turgor. *Plant, Cell & Environment* **39**:2014–2026.

Roose T, Fowler AC. 2004. A model for water uptake by plant roots. *Journal of Theoretical Biology* **228**:155–171.

Sabot MEB, De Kauwe MG, Pitman AJ, Medlyn BE, Verhoef A, Ukkola AM, Abramowitz G. 2020. Plant profit maximization improves predictions of European forest responses to drought. *The New Phytologist* **226**:1638–1655.

Sack L, Holbrook NM. 2006. Leaf hydraulics. *Annual Review of Plant Biology* **57**:361–381.

Sack L, Scoffoni C, Johnson DM, Buckley TN, Brodribb TJ. 2015. The anatomical determinants of leaf hydraulic function. In: Hacke U, ed. *Functional and ecological xylem anatomy*. Cham: Springer International Publishing, 255–271.

Saint Cast C, Meredieu C, Défossez P, Pagès L, Danjon F. 2020. Clustering of *Pinus pinaster* coarse roots, from juvenile to mature stage. *Plant and Soil* **457**:185–205.

Schenk HJ, Steppe K, Jansen S. 2015. Nanobubbles: a new paradigm for air-seeding in xylem. *Trends in Plant Science* **20**:199–205.

Schnepf A, Leitner D, Landl M, Lobet G, Mai TH, Morandage S, Sheng C, Zörner M, Vanderborght J, Vereecken H. 2018. CRootBox: a structural-functional modelling framework for root systems. *Annals of Botany* **121**:1033–1053.

Schoppach R, Wauthelet D, Jeanguenin L, Sadok W, Schoppach R, Wauthelet D, Jeanguenin L, Sadok W. 2013. Conservative water use under high evaporative demand associated with smaller root metaxylem and limited transmembrane water transport in wheat. *Functional Plant Biology* **41**:257–269.

Schulte PJ. 2012. Computational fluid dynamics models of conifer bordered pits show how pit structure affects flow. *The New Phytologist* **193**:721–729.

Scoffoni C, Albuquerque C, Brodersen CR, Townes SV, John GP, Bartlett MK, Buckley TN, McElrone AJ, Sack L. 2017. Outside-xylem vulnerability, not xylem embolism, controls leaf hydraulic decline during dehydration. *Plant Physiology* **173**:1197–1210.

Scoffoni C, Albuquerque C, Cochard H, Buckley TN, Fletcher LR, Caringella MA, Bartlett M, Brodersen CR, Jansen S, McElrone AJ, Sack L. 2018. The causes of leaf hydraulic vulnerability and its influence on gas exchange in *Arabidopsis thaliana*. *Plant Physiology* **178**:1584–1601.

Scoffoni C, Chatelet DS, Pasquet-Kok J, Rawls M, Donoghue MJ, Edwards EJ, Sack L. 2016. Hydraulic basis for the evolution of photosynthetic productivity. *Nature Plants* **2**:16072.

Scoffoni C, Sack L, Ort D. 2017. The causes and consequences of leaf hydraulic decline with dehydration. *Journal of Experimental Botany* **68**:4479–4496.

Sevanto S, Nikinmaa E, Riikonen A, Daley M, Pettijohn JC, Mikkelsen TN, Phillips N, Holbrook NM. 2008. Linking xylem diameter variations with sap flow measurements. *Plant and Soil* **305**:77–90.

Sevanto S, Vesala T, Perämäki M, Nikinmaa E. 2002. Time lags for xylem and stem diameter variations in a Scots pine tree. *Plant, Cell & Environment* **25**:1071–1077.

Sevilem I, Miyashima S, Helariutta Y. 2013. Cell-to-cell communication via plasmodesmata in vascular plants. *Cell Adhesion & Migration* **7**:27–32.

Sheehy JE, Mitchell PL, Durand J-L, Gastal F, Woodward FI. 1995. Calculation of translocation coefficients from phloem anatomy for use in crop models. *Annals of Botany* **76**:263–269.

Simunek J, Van Genuchten MT, Sejna M. 2005. The HYDRUS-1D software package for simulating the one-dimensional movement of water, heat, and multiple solutes in variably-saturated media. *University of California-Riverside Research Reports* **3**:1–240.

Sinclair TR, Devi J, Shekoofa A, Choudhary S, Sadok W, Vadez V, Riar M, Rufty T. 2017. Limited-transpiration response to high vapor pressure deficit in crop species. *Plant Science* **260**:109–118.

Slatyer R. 1967. *Plant–water relationships*. London and New York: Academic Press.

Smith KC, Magnuson CE, Goeschl JD, DeMichele DW. 1980. A time-dependent mathematical expression of the Münch hypothesis of phloem transport. *Journal of Theoretical Biology* **86**:493–505.

Spanner DC. 1951. The Peltier effect and its use in the measurement of suction pressure. *Journal of Experimental Botany* **2**:145–168.

Sperry JS, Hacke UG, Pittermann J. 2006. Size and function in conifer tracheids and angiosperm vessels. *American Journal of Botany* **93**:1490–1500.

Sperry JS, Sullivan JE. 1992. Xylem embolism in response to freeze-thaw cycles and water stress in ring-porous, diffuse-porous, and conifer species. *Plant Physiology* **100**:605–613.

Sperry JS, Tyree MT. 1988. Mechanism of water stress-induced xylem embolism. *Plant Physiology* **88**:581–587.

Sperry JS, Venturas MD, Anderegg WRL, Mencuccini M, Mackay DS, Wang Y, Love DM. 2017. Predicting stomatal responses to the environment from the optimization of photosynthetic gain and hydraulic cost. *Plant, Cell & Environment* **40**:816–830.

Sperry JS, Wang Y, Wolfe BT, Mackay DS, Anderegg WR, McDowell NG, Pockman WT. 2016. Pragmatic hydraulic theory predicts stomatal responses to climatic water deficits. *The New Phytologist* **212**:577–589.

Steppe K. 2018. The potential of the tree water potential. *Tree Physiology* **38**:937–940.

Steppe K, De Pauw DJ, Lemeur R, Vanrolleghem PA. 2006. A mathematical model linking tree sap flow dynamics to daily stem diameter fluctuations and radial stem growth. *Tree Physiology* **26**:257–273.

Steppe K, Lemeur R. 2007. Effects of ring-porous and diffuse-porous stem wood anatomy on the hydraulic parameters used in a water flow and storage model. *Tree Physiology* **27**:43–52.

Steppe K, Sterck F, Deslauriers A. 2015. Diel growth dynamics in tree stems: linking anatomy and ecophysiology. *Trends in Plant Science* **20**:335–343.

Steudle E. 2000a. Water uptake by plant roots: an integration of views. *Plant and Soil* **226**:45–56.

Steudle E. 2000b. Water uptake by roots: effects of water deficit. *Journal of Experimental Botany* **51**:1531–1542.

Steudle E, Peterson CA. 1998. How does water get through roots? *Journal of Experimental Botany* **322**:775–788.

Stroock AD, Pagay VV, Zwieniecki MA, Michele Holbrook N. 2014. The physicochemical hydrodynamics of vascular plants. *Annual Review of Fluid Mechanics* **46**:615–642.

Sulis M, Couvreur V, Keune J, Cai G, Trebs I, Junk J, Shrestha P, Simmer C, Kollet SJ, Vereecken H, Vanderborght J. 2019. Incorporating a root water uptake model based on the hydraulic architecture approach in terrestrial systems simulations. *Agricultural and Forest Meteorology* **269–270**, 28–45.

Tardieu F. 2012. Any trait or trait-related allele can confer drought tolerance: just design the right drought scenario. *Journal of Experimental Botany* **63**:25–31.

Tardieu F, Davies WJ. 1993. Integration of hydraulic and chemical signalling in the control of stomatal conductance and water status of droughted plants. *Plant, Cell & Environment* **16**:341–349.

Tardieu F, Granato ISC, Van Oosterom EJ, Parent B, Hammer GL. 2020. Are crop and detailed physiological models equally 'mechanistic' for predicting the genetic variability of whole-plant behaviour? The nexus between mechanisms and adaptive strategies. *In Silico Plants* **2**:diaa011; doi:10.1093/insilicoplants/diaa011

Tardieu F, Simonneau T, Parent B. 2015. Modelling the coordination of the controls of stomatal aperture, transpiration, leaf growth, and abscisic acid: update and extension of the Tardieu–Davies model. *Journal of Experimental Botany* **66**:2227–2237.

Tardieu F, Tuberosa R. 2010. Dissection and modelling of abiotic stress tolerance in plants. *Current Opinion in Plant Biology* **13**:206–212.

Thompson MV, Holbrook NM. 2003. Application of a single-solute non-steady-state phloem model to the study of long-distance assimilate transport. *Journal of Theoretical Biology* **220**:419–455.

Thornley JHM. 1998. *Grassland dynamics: an ecosystem simulation model*. Wallingford (UK) and New York: CAB International.

Thornley JHM, Johnson IR. 1990. *Plant and crop modelling: a mathematical approach to plant and crop physiology*. Oxford: Oxford University Press.

Tuzet A, Perrier A, Leuning R. 2003. A coupled model of stomatal conductance, photosynthesis and transpiration. *Plant, Cell & Environment* **26**:1097–1116.

Tyree MT. 2003. Hydraulic limits on tree performance: transpiration, carbon gain and growth of trees. *Trees* **17**:95–100.

Tyree MT, Zimmermann MH. 2002. *Xylem structure and the ascent of sap*, 2nd edn. Berlin, Heidelberg: Springer-Verlag.

van Bel AJE. 2003. The phloem, a miracle of ingenuity: the phloem, a miracle of ingenuity. *Plant, Cell & Environment* **26**:125–149.

van den Honert TH. 1948. Water transport in plants as a catenary process. *Discussions of the Faraday Society* **3**:146–153.

Vandeleur RK, Mayo G, Shelden MC, Gilliham M, Kaiser BN, Tyerman SD. 2009. The role of plasma membrane intrinsic protein aquaporins in water transport through roots: diurnal and drought stress responses reveal different strategies between isohydric and anisohydric cultivars of grapevine. *Plant Physiology* **149**:445–460.

Vandeleur RK, Sullivan W, Athman A, Jordans C, Gilliham M, Kaiser BN, Tyerman SD. 2014. Rapid shoot-to-root signalling regulates root hydraulic conductance via aquaporins. *Plant, Cell & Environment* **37**:520–538.

Venturas MD, MacKinnon ED, Dario HL, Jacobsen AL, Pratt RB, Davis SD. 2016. Chaparral shrub hydraulic traits, size, and life history types relate to species mortality during california's historic drought of 2014. *PLoS One* **11**:e0159145.

Venturas MD, Sperry JS, Hacke UG. 2017. Plant xylem hydraulics: what we understand, current research, and future challenges. *Journal of Integrative Plant Biology* **59**:356–389.

Vetterlein D, Doussan C. 2016. Root age distribution: how does it matter in plant processes? A focus on water uptake. *Plant and Soil* **407**:145–160.

Wang DR, Venturas MD, Mackay DS, Hunsaker DJ, Thorp KR, Gore MA, Pauli D. 2020. Use of hydraulic traits for modeling genotype-specific acclimation in cotton under drought. *The New Phytologist* **228**:898–909.

Watanabe Y, Kabuki T, Kakehashi T, Kano-Nakata M, Mitsuya S, Yamauchi A. 2020. Morphological and histological differences among three types of component roots and their differential contribution to water uptake in the rice root system. *Plant Production Science* **23**:191–201.

Wolf A, Anderegg WR, Pacala SW. 2016. Optimal stomatal behavior with competition for water and risk of hydraulic impairment. *Proceedings of the National Academy of Sciences of the United States of America* **113**:E7222–E7230.

Xiong D, Nadal M. 2020. Linking water relations and hydraulics with photosynthesis. *The Plant Journal* **101**:800–815.

Yin X, Struik PC. 2010. Modelling the crop: from system dynamics to systems biology. *Journal of Experimental Botany* **61**:2171–2183.

Zarebanadkouki M, Trtik P, Hayat F, Carminati A, Kaestner A. 2019. Root water uptake and its pathways across the root: quantification at the cellular scale. *Scientific Reports* **9**:12979.

Zhou X-R., Schnepf A, Vanderborght J, Leitner D, Lacointe A, Vereecken H, Lobet G. 2020. CPlantBox, a whole-plant modelling framework for the simulation of water- and carbon-related processes. *In Silico Plants* **2**:diaa001; doi:10.1093/insilicoplants/diaa001

Zhu GL, Steudle E. 1991. Water transport across maize roots: simultaneous measurement of flows at the cell and root level by double pressure probe technique. *Plant Physiology* **95**:305–315.

Zimmermann D, Reuss R, Westhoff M, Gessner P, Bauer W, Bamberg E, Bentrup FW, Zimmermann U. 2008. A novel, non-invasive, online-monitoring, versatile and easy plant-based probe for measuring leaf water status. *Journal of Experimental Botany* **59**:3157–3167.

Zweifel R, Item H, Häsler R. 2001. Link between diurnal stem radius changes and tree water relations. *Tree Physiology* **21**:869–877.

Zwieniecki MA, Thompson MV, Holbrook NM. 2002. Understanding the hydraulics of porous pipes: tradeoffs between water uptake and root length utilization. *Journal of Plant Growth Regulation* **21**:315–323.